Progress in Oceanography 240 (2026) 103615

Contents lists available at ScienceDirect

Progress in Oceanography

journal homepage: www.elsevier.com/locate/pocean

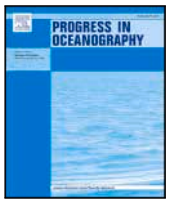

How contrasted environments in the Humboldt Current System, Pacific Warm Pool and South Pacific Gyre, shape contrasted ecosystems. A modelling approach using APECOSM

Laureline Dalaut *, Nicolas Barrier, Matthieu Lengaigne, Olivier Maury

MARBEC, Univ. Montpellier, CNRS, Ifremer, IRD, Sète, France

ARTICLE INFO

Keywords:
APECOSM
Mechanistic ecosystem model
Ecosystem structure
Ecosystem function
Pelagic ecosystem
Trophic interactions
Humbold Current System
Pacific Warm Pool
South Pacific Gyre

ABSTRACT

Pelagic ecosystems exhibit a strong regional heterogeneity, driven by physical and biogeochemical characteristics. Using the global 3D marine ecosystem model APECOSM, we simulate six high-trophic-level communities, capturing their size structure, spatial distribution, and trophic interactions up to 1,000 metres depth. We examine how different environments shape their contrasting organisation and interactions in three Pacific Ocean regions: the productive Humboldt Current System, the oligotrophic South Pacific Gyre, and the thermally stratified Pacific Warm Pool.

Simulations reveal strong regional contrasts in ecosystem responses. In the Humboldt, high primary production supports important biomass of small coastal pelagic fish. Seasonal warming enables tuna to forage in these productive waters, while low-oxygen conditions restrict the vertical range and abundance of mesopelagic organisms and concentrate epipelagic organisms close to the surface. In the Warm Pool, apex predators remain abundant despite low primary production, thanks to efficient trophic transfer and biomass import from neighbouring regions. Seamounts concentrate mesopelagic organisms into shallow layers, making them accessible to epipelagic predators. In contrast, the South Pacific Gyre supports sparse, imported high-trophic-levels with limited trophic coupling and strong intra-community predation. We quantify regional differences in trophic transfer efficiency and network complexity, identifying thresholds below which high-trophic-levels collapse.

These findings illustrate the emergent plasticity of pelagic ecosystems and the importance of bottom-up control of high-trophic-level biomass. They emphasise the importance of temperature, transport, light and oxygen in modulating horizontal and vertical distributions, controlling the co-occurrence of predators and prey, and influencing the formation of schools, ultimately impacting trophic interactions and community assemblages.

1. Introduction

The open ocean hosts rich pelagic ecosystems shaped by the interplay of physical, biogeochemical, and ecological processes (e.g. see Dalaut et al. 2025). However, these processes do not act uniformly across the global ocean; instead, they generate substantial regional variability in ecosystem structure and function. Understanding how environmental heterogeneity translates into distinct pelagic ecosystem configurations remains a key challenge in marine ecology and global ecosystem modelling. Among all ocean basins, the Pacific Ocean, the largest on the planet, exemplifies this diversity, ranging from nutrient-rich upwelling zones to oligotrophic gyres and stratified equatorial waters. In this study, we focus on three hydrologically and ecologically distinct regions of the Pacific: the Humboldt Current System (HCS), the Pacific Warm Pool (PWP), and the South Pacific Gyre (SPG). The HCS is a highly productive eastern boundary upwelling system that supports important fisheries of small pelagic fish and dense aggregations of warm-blooded predators (Bakun and Weeks, 2008). In contrast, the SPG is an oligotrophic region, characterised by low primary production dominated by small nitrogen-fixing organisms and very low biomass of high trophic levels. The PWP, despite its limited primary productivity (Halm et al., 2012; Barber and Chavez, 1991), supports a high diversity of marine life, including large tropical top predators such as tuna, making it one of the world's most productive tuna fishing grounds (Williams and Terawasi, 2009; Langley et al., 2009).

Representing such contrasting regional ecosystem structures and

* Corresponding author.
E-mail address: laureline.dalaut@ird.fr (L. Dalaut).

https://doi.org/10.1016/j.pocean.2025.103615
Received 24 July 2025; Received in revised form 21 October 2025; Accepted 31 October 2025
Available online 7 November 2025

functions using the generic design and rules of a global marine ecosystem model is a major challenge. Capturing the key processes and their interactions at different temporal and spatial scales without excessive parametrisation and computational cost also requires a careful modelling strategy (Fulton et al., 2003). APECOSM (Apex Predators ECOSystem Model, e.g. Maury, 2010; Maury and Poggiale, 2013) addresses this by adopting a mechanistic, three-dimensional, trait-based and size-structured approach that explicitly represents the main processes responsible for the structure and dynamics of marine ecosystems. The model represents basic biological and ecological processes at the individual level, based on a small set of first principles and simple assumptions. This allows the macroscopic structure and function of the ecosystem to emerge from the interactions between individual dynamics and the physical–biogeochemical environment.

Configuring APECOSM involves defining a set of archetypal functional communities, for which a limited number of parameters are required (e.g. temperature ranges, light sensitivities, maximum species length ranges, predator/prey size ratios, and diurnal or nocturnal behaviours). This approach captures the adaptive complexity and diversity of key ecosystem responses to the environmental conditions, enables mechanistic exploration of high trophic level dynamics, and ensures reasonable computational costs (e.g. Dalaut et al. 2025).

This paper aims to evaluate whether APECOSM can reproduce the structural and functional diversity of pelagic ecosystems in these three contrasting Pacific regions, and to provide a mechanistic understanding of their ecological uniqueness. For this purpose, we use the six high trophic level (HTL) community configuration described and assessed against observations in Dalaut et al. (2025) to explore how regional environmental heterogeneity, particularly in temperature, productivity, stratification, oxygenation, and seasonality, shapes tridimensional biomass distribution, size spectra and emergent trophic functioning. By conducting a cross-regional comparative analysis, we identify key ecological processes, understand how pelagic communities respond to varying environmental drivers in each system and how regional systems interact. In light of empirical studies published in the literature, we discuss our results and how our simulations help explain observations.

The paper is organised as follows : Section 2 presents the model and its configuration (Section 2.1), as well as the simulation setup (Section 2.2). Section 3 explores each specific region to highlight their particularities in terms of size and community structure, three-dimensional spatial distribution as well as emergent trophic interactions. Finally, Section 4 provides a brief summary and discussion of the contribution of these results to our understanding of marine ecosystems structure and function.

2. Method and tools

2.1. The APECOSM model and its configuration

This study uses the marine ecosytem model APECOSM (Apex Predators ECOSystem Model), which employs a mechanistic approach based on first principles. APECOSM integrates the dynamic energy budget theory (Kooijman, 2010) and a trait-based approach (Maury and Poggiale, 2013) with a limited set of elementary assumptions formulated at the individual level to describe the 3D dynamics and trophic interactions of size-structured HTLs communities (e.g. Maury, 2010). APECOSM is driven by the three-dimensional physical and biochemical fields outputted by the physical ocean model NEMO-v3.2 (Madec, 2015) coupled to the biogeochemical model PISCES-v2 (Aumont et al., 2015). The three-dimensional environmental forcing variables used in APECOSM include temperature, currents, dissolved oxygen concentration, light and concentrations of the low trophic level (LTL) functional groups represented in PISCES (i.e. flagellates and diatoms, micro- and meso-zooplankton, small and large particulate carbon).

APECOSM allows the simulation of distinct interactive communities that share the same generic structure and functioning, but differ in a small number of key parameters. In this study, we use the six HTL communities configuration of the model, which is described and evaluated in Dalaut et al. (2025). This configuration allows the simulation of the following communities:

1. **The tropical tuna community** includes all large epipelagic tropical top predators, including tropical tunas such as yellowfin tuna (*Thunnus albacares*) and skipjack tuna (*Katsuwonus pelamis*). This community inhabits warm, open-ocean waters and is expected to stabilise the pelagic food chain through predation on smaller, more variable species (Maury, 2017).
2. **The small coastal pelagic community** inhabits productive and cold ocean regions, particularly the Eastern Boundary Upwelling Systems (EBUS ; including the Benguela, California, Canary and Humboldt upwellings). It includes species that are mostly plankton feeders (e.g. sardines, anchovies, sprats).
3. **The small and medium epipelagic community** represents a wide range of fish and non-fish nektonic species living in the open ocean and includes all epipelagic species not classified as small coastal pelagics or tropical tunas. It includes for instance sardinellas (*Sardinella spp.*), Chilean jack mackerel (*Trachurus murphyi*), chub mackerel (*Scomber japonicus*) or pandora (*Pagellus erythrinus*).
4. **The mesopelagic migrant community** represents organisms that forage at night in the epipelagic zone and migrate to deeper mesopelagic waters during the day. It includes fish species such as lanternfishes (*Myctophidae*, *Notoscopelidae*), lightfishes (*Phosichthyidae*), or hatchetfishes (*Sternoptychidae*) but also other organisms like squids or gelatinous organisms.
5. **The mesopelagic resident community** represents all the organisms that permanently reside at depths between 200 m and 1000 m. It includes a wide variety of fish and cephanlopod species such as the ubiquitous genus *Cyclothone*, *Stomiidae*, *Alepocephalidae* or *Ceratioidea*.
6. **The mesopelagic-feeding tuna community** represents the ecological specificity of bigeye tuna (*Thunnus obesus*) and other top predator species with similar behaviour (e.g. swordfish *Xiphias gladius* for instance), which inhabit the epipelagic zone but forage during the day in the mesopelagic zone when they are large.

2.2. Simulation setup

Our simulation is initialised with an extended spin-up, using the outputs of a NEMO-PISCES simulation forced with linearly detrended atmospheric inputs derived from the JRA-55 atmospheric reanalysis (Kobayashi et al., 2015) over the period 1958–2022. The detrending methodology employed for the spin-up preserves interannual to multidecadal signals while effectively removing long-term climate change signals from the forcing. Further details on this methodology can be found in Lengaigne et al. (2024). The 65-year spin-up period ensures that each community reaches a quasi-stationary state.

Using the last day of this spin-up simulation as initial state, APECOSM was then run using the outputs of a NEMO-PISCES simulation forced with the original (i.e. not detrended) JRA-55 atmospheric fluxes over the period 1958–2022. This hindcast simulation includes both realistic variability and climate change signals, and serves as a basis for the analyses presented here.

3. The emerging structure and functioning of the ecosystem in each region

This section provides an in-depth analysis of the size and tridimensional spatial structure as well as trophic functioning of the ecosystem in each region (see Fig. 1), as they emerge in our APECOSM simulation. Section 3.1, examines the HCS, highlighting the diverse physical

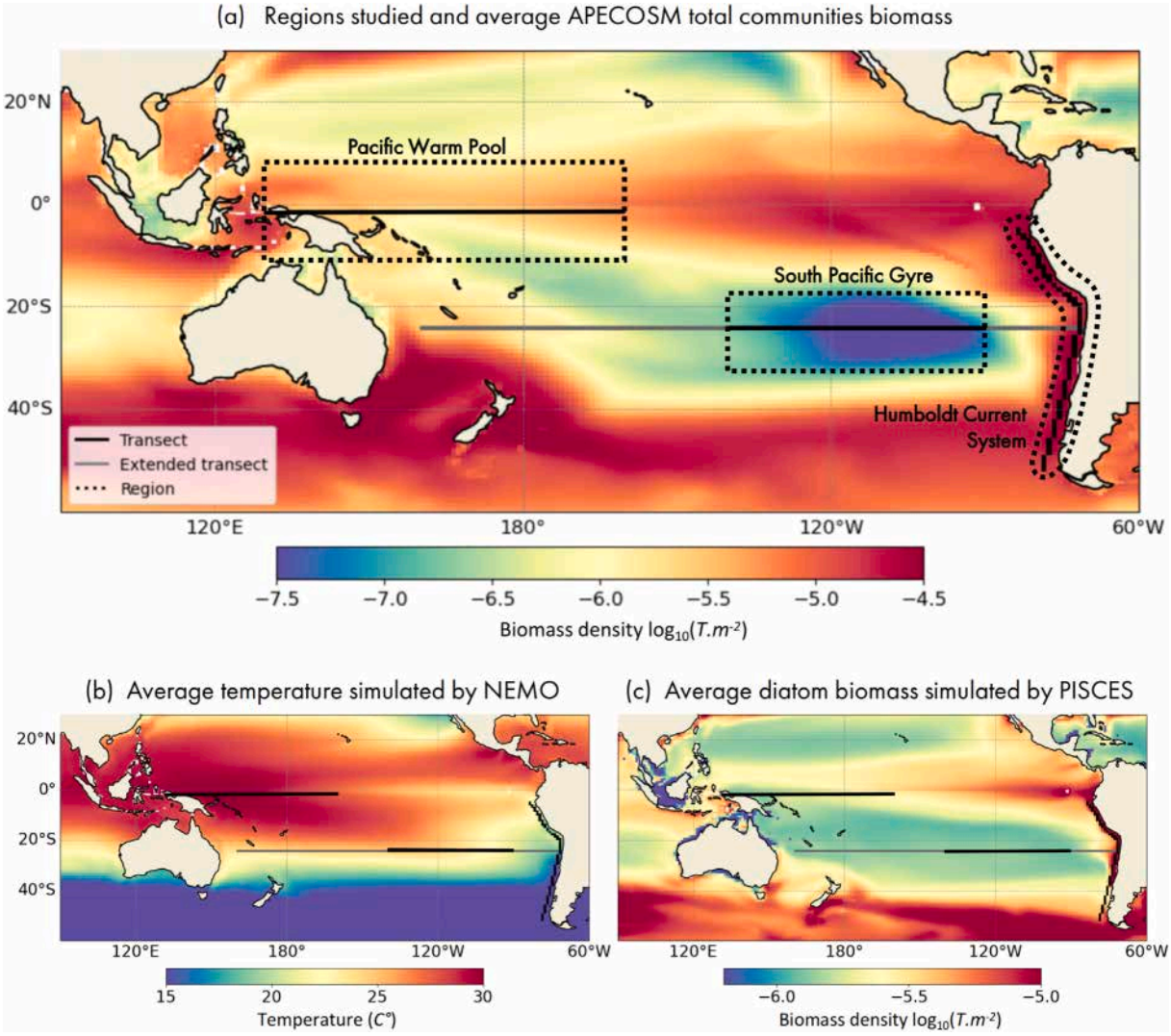

Fig. 1. Map of the Pacific regions studied. (a) Total biomass of the six APECOSM high trophic level communities with the locations of the three regions studied: the Pacific Warm Pool, the South Pacific Gyre, and the Humboldt Current System. The transects used in this study are shown as black solid lines. An additional extended transect (grey line) is included for the South Pacific Gyre to examine the transition from non-gyre to gyre conditions. The dotted lines indicate the boxes over which spatially integrated metrics are calculated. (b) Mean sea surface temperature from the NEMO model, (c) mean vertically integrated diatom biomass from the PISCES model. All figures represent averages over the 2000–2020 period.

and biogeochemical processes that shape the ecological dynamics of different communities. In Section 3.2, we turn to the PWP to show how, despite low-productivity, this region maintains a relatively diverse assemblage of communities. Finally, in Section 3.3, we investigate the SPG and its surroundings to explore the ecological transition from a productive coastal system to an oligotrophic gyre environment.

3.1. The Humboldt Current System

In the HCS, a range of physical and biogeochemical processes, described in Section 3.1.1, interact to shape ecosystem structure and function. Section 3.1.2 examines the size spectrum of the different communities in the HCS in comparison to the global average. We then analyse how bottom-up control affects the small coastal pelagic community in the region (Section 3.1.3). Next, we assess the influence of the oxygen minimum zone on mesopelagic communities, and its broader implications for ecosystem structure and trophic functioning (Section 3.1.4). Then we explore how seasonal environmental variability drives the seasonal presence of tunas along the Peruvian coast (Section 3.1.5). Finally, we analyse how these structural features shape the rich trophic network of the HCS and we demonstrate that this region acts as a net biomass 'source' (Section 3.1.6).

3.1.1. The Humboldt Current System: A productive upwelling zone

The HCS is one of the four Eastern Boundary Upwelling Systems (EBUS), along with the Benguela, California, and Canary upwellings. The HCS originates in the southeastern Pacific and stems from the West Wind Drift (WWD) at around 40° S. It forms part of the eastward-flowing South Pacific Current. This current bifurcates near southern Chile and flows northwards along the Chilean and Peruvian coasts, steered by the Coriolis force, as part of the SPG (Hill, 1963). The interaction between persistent southeasterly trade winds and the Earth's rotation induces the upwelling of cold, nutrient-rich waters. This upwelling is localised on the continental shelf along the coasts of Peru and Chile. It is continuous and aseasonal off Peru and northern Chile, but more seasonal further south (Kämpf and Chapman, 2016). Thanks to this upwelling, the northern HCS off Peru is one of the most productive marine ecosystem in the world, supporting very high plankton concentrations and abundant small pelagic fish stocks (Echevin et al., 2014). Although it covers less than 0.1% of the ocean's surface, it accounts for approximately 7% of the world's fish catch, driven primarily by the

anchoveta *Engraulis ringens* fishery (FAO, 2021). The region's intense fishing activity is facilitated by the presence of an oxygen minimum zone (OMZ), which acts as a vertical barrier that concentrates marine organisms into surface layers, making them more accessible to commercial fisheries. This OMZ results from a combination of high oxygen demand associated with sub-surface organic matter decomposition and poor water column ventilation (Fuenzalida et al., 2009). The OMZ is deeper off the northern coast of Peru and becomes shallower southward (Pizarro et al., 2002).

3.1.2. High biomass and size-structured variability

The size spectra of marine ecosystems exhibit strong regularities reflecting the biological and ecological importance of size in controlling the flow and dissipation of energy through ecosystems (Andersen et al., 2016; Blanchard et al., 2017). It has been suggested that oligotrophic systems have steeper size-spectrum slopes (Jennings and Mackinson, 2003). Here, we examine the size-spectrum simulated by APECOSM in the HCS and interpret it based on the environment's physics and biogeochemistry and published literature.

Fig. 2 presents the global and regional size spectra of LTL and HTL communities simulated by PISCES and APECOSM. In the HCS, the biomass of small coastal pelagics is exceptionally high (Fig. 2b), relative to the global average (Fig. 2a), particularly at small sizes, reaching values comparable to mesopelagic communities. Between sizes of 0.1 g and 1 g (1.86 to 4 cm), their biomass even exceeds that of mesopelagics. This pattern in the model results from the high plankton concentration, which accelerates juvenile growth and improves larval survival. Additionally, the density-dependent regulation by schools, which control predation mortality and density-dependent access to food, is not yet active in these early life stages (Maury, 2017).

Interestingly, the typical dominance of mesopelagic residents over migrants is reversed in the HCS, where migrant biomass exceeds resident biomass. This inversion stems from the presence of an intense OMZ that overlaps the depth range usually occupied by mesopelagic resident species and limits their vertical distribution (e.g. Dalaut et al., 2025; see 3.1.4).

Tuna communities in the HCS also display distinct size structure compared to the global pattern. Small tuna are nearly absent, with biomass increasing only gradually with body mass, peaking at intermediate sizes (3.2 g to 2.3 kg, equivalent to 5.5 to 45 cm) before declining. This is because tropical tuna only spawn in waters that are warmer than 24–26 °C (Fujioka et al., 2024; Fonteneau, 1997). Consequently, only intermediate size classes are abundant in the region, while larger individuals tend to occupy more offshore waters, consistent with observations (Fuller et al., 2021).

The pronounced environmental seasonality of the HCS leads to marked seasonal oscillations in size spectra (Fig. 2b). These oscillations primarily affect organisms under 10 g (approximately 9 cm) in the small coastal pelagic community and in the two mesopelagic communities. Such patterns likely arise from seasonal variations in temperature and primary production at high latitudes, resulting in fluctuation in small organisms' biomass (Maury et al., 2007; Le Mézo et al., 2016), such as simulated here and observed for anchovies and sardines (Cerna et al., 2022), which rely heavily on LTL resources. For larger predators, such as tropical and mesopelagic-feeding tunas, seasonal oscillations extend up to 30 kg and 1.25 m. This suggests seasonal incursions of tropical predators into the HCS during the warm season (Alheit and Niquen, 2004).

3.1.3. Bottom-up control of the small coastal pelagic community

One of the most notable features of the HCS is the very high density of small coastal pelagics. In this section, we analyse the spatial distribution and functional importance of this community based on the results presented in Fig. 3: the vertical distribution of the small coastal pelagic community in 3a, the trophic flux (i.e. the total depth- and size-integrated flux of energy eaten by a given community) it generates as a predator in 3b, and its latitudinal distribution in relation to primary production in 3c.

The simulated small coastal pelagic community reaches considerable biomass levels all along the studied transect (Fig. 3a) from 6 °S to 43 °S. This is consistent with observations and aligns with the fact that the HCS ecosystem supports the world's largest production of small pelagic fish, primarily anchoveta (FAO, 2021).

In the model, this community is predominantly concentrated in the upper 50 m of the water column, with peak biomass around 20 m depth. This zone is characterised by high plankton abundance and elevated oxygen concentrations. The distribution and the opportunistic diet of the small coastal pelagic community are mainly driven by the availability of the different planktonic groups. Between 6 °S and 34 °S, their diet consists of mesozooplankton, diatoms, and microzooplankton. Around 25° S and south of 40 °S, it shifts towards a predominantly mesozooplankton-based regime (Fig. 3b). Anchoveta distribution and dynamics in the region are known to be largely driven by bottom-up controls through plankton availability (Ayón et al., 2008). This species, implicitly represented in the small coastal pelagic community, benefits from the productive upwelling conditions. Access to high concentrations of zooplankton at the shelf break (Bertrand et al., 2008b), and reduced predation and competition due to the OMZ-driven exclusion of hypoxia-intolerant organisms, further enhance its success (Bertrand et al., 2011).

The spatial distribution of the small coastal pelagic biomass simulated by APECOSM (Fig. 3c) matches closely the distribution of the anchovy (*Engraulis ringens*) fishery, with peak landing north of 40 °S (Alheit and Niquen, 2004; Cubillos et al., 2007). The most productive fisheries are located off north-central Peru (6°–15 °S), where persistent trade winds drive year-round upwelling and high primary production, particularly of large diatoms (Pennington et al., 2006). This area is flanked by a transboundary fishery off southern Peru and northern Chile (16°–27 °S), and a less productive sector off central and southern Chile (34°–40 °S) (Alheit and Niquen, 2004; Cubillos et al., 2007).

However, in low-latitude regions from 6 °S to 10 °S the model simulates unexpectedly low small coastal pelagic biomass (Fig. 3c). Here, food is not limiting, but warm temperatures exceed the community's upper thermal tolerance (21 °C) in the model with temperatures at 20 m depth reaching 25 °C from February to April. This contrasts with observations showing that inshore waters in these low-latitude regions actually remain at around 21 °C, with fisheries present in these zones during the austral summer (Bertrand et al., 2008a; Diaz et al., 2013). The discrepancy likely stems from the coarse spatial resolution of the NEMO-PISCES model, which misrepresents the nearshore fine-scale heterogeneity and intensity of the upwelling, likely leading to overestimated surface temperatures and underestimated small coastal pelagic biomass in this region compared to central Chile.

Around 25 °S, the model shows a decrease in small coastal pelagic related to lower LTL concentrations (Fig. 3c). This region corresponds to the narrow continental shelf in northern Chile (Karstensen and Ulloa, 2009), which limits nutrient retention and mixing in the euphotic zone and thus lowers LTL production (Tornquist et al., 2024). Conversely, central Chile (30 °S–40 °S) benefits from strong eddies that enhance nutrient upwelling and phytoplankton biomass (Thiel et al., 2007). Despite our low-resolution models being unable to simulate these small-scale features, APECOSM simulates high small coastal epipelagic biomass (Fig. 3c), consistently with observations of high anchovy, herring, and jack mackerel concentrations in this area (Hasan and Halwart, 2009).

Further south (40°–52 °S), freshwater inputs from river discharge and precipitation enhance water column stratification, thereby limiting the mixing of nutrients and phytoplankton productivity (Aracena et al., 2011; Tornquist et al., 2024). In APECOSM, the lower coastal pelagic biomass in this region reflects lower primary production and colder temperatures.

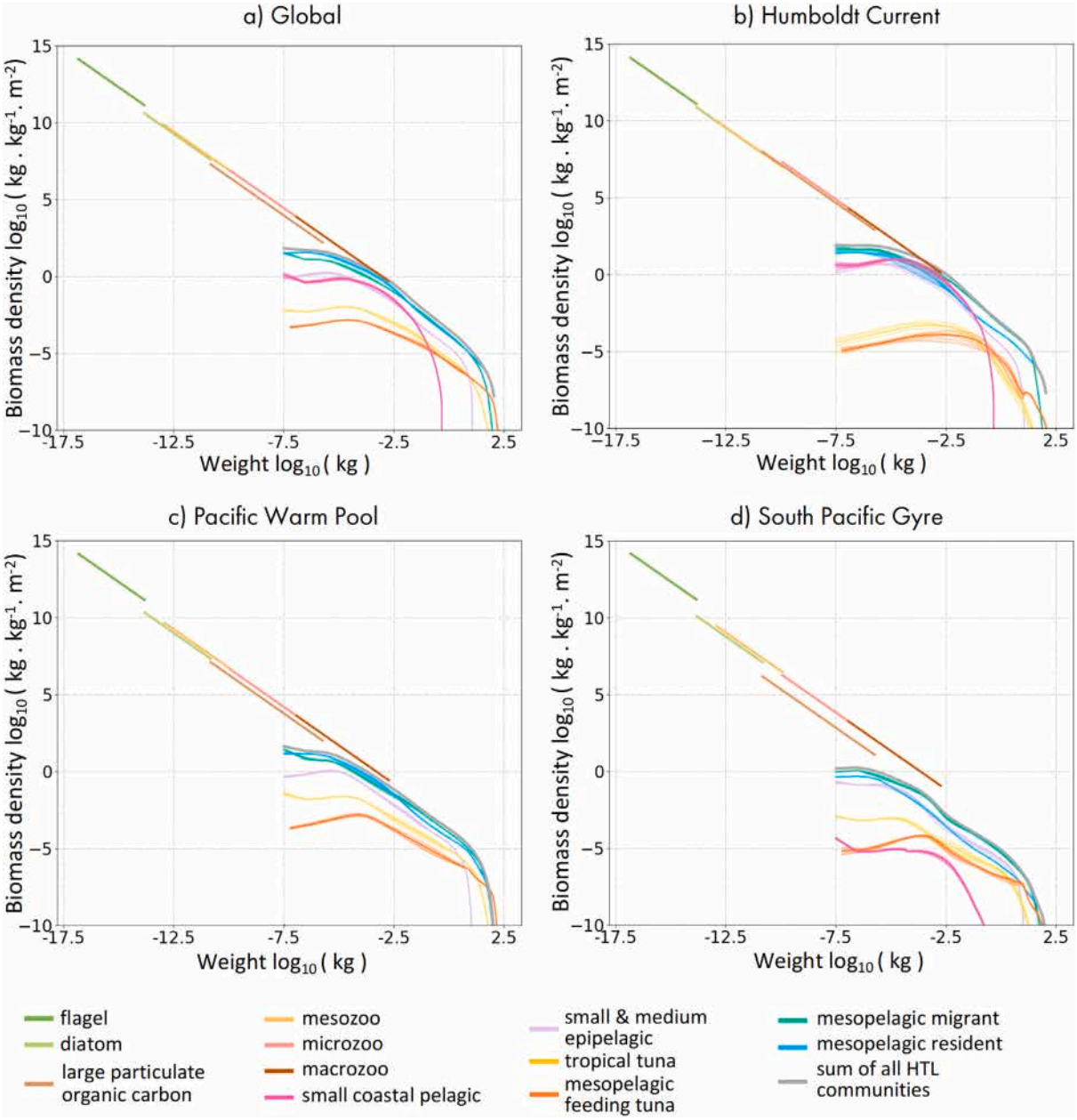

Fig. 2. Size spectra across regions. Average biomass density size spectra from 2000 to 2020 at the global scale (a), in the Humboldt Current System (b), in the Pacific Warm Pool (c), and in the South Pacific Gyre (d). The straight line represents low trophic level organisms from the PISCES model. The bold grey line shows the total annual biomass spectrum simulated by APECOSM. Colours represent different high trophic level communities: purple for small and medium epipelagics, yellow for tropical tunas, green for mesopelagic migrants, blue for mesopelagic residents, orange for mesopelagic-feeding tunas, and pink for small coastal pelagics. Thin lines indicate monthly biomass spectra for each community.

3.1.4. The oxygen minimum zone differentially affects mesopelagic communities

The northern HCS, off the coast of Peru, hosts one of the most intense and shallowest OMZ in the world (Valdés et al., 2021), characterised by a steep oxycline and hypoxic waters (defined here as regions where oxygen concentration falls below 1 ml l^{-1}) extending to several hundred of metres. While the OMZ is a barrier to many organisms, it also serves as a refuge and feeding ground for species adapted to low-oxygen conditions (Wishner et al., 1995; Eduardo et al., 2024). In our APECOSM simulation, mesopelagic communities, which occupy depths between 200 and 1000 m, are particularly affected by the presence of the OMZ. As shown in Figs. 3a and 3c, simulated mesopelagic migrant organisms are broadly distributed between 200 to 600 m along the transect, but their biomass is significantly reduced near 6 °S, between 24 °S and 28 °S, and south of 38 °S. In the 18 °S and 28 °S sector, where the OMZ is particularly shallow, their daytime vertical distribution is compressed around 300 m, while outside these regions, they occupy deeper layers. The trophic flux to these organisms is very high from 6 °S to 52 °S, with a diet dominated by mesozooplankton and macrozooplankton, and to a lesser extent, mesopelagic migrants, small and medium epipelagics and small coastal pelagics (Fig. 3d).

As for the small coastal pelagic community, the simulated horizontal distribution of the mesopelagic migrant community shows two main areas of high biomass in the North and South, separated by a poorer zone (Fig. 3c). This suggests that their distribution is primarily driven by prey availability rather than oxygen constraints. It has been shown that mesopelagic migrants tolerate hypoxic conditions during daytime by reducing their metabolic activity or employing anaerobic metabolic

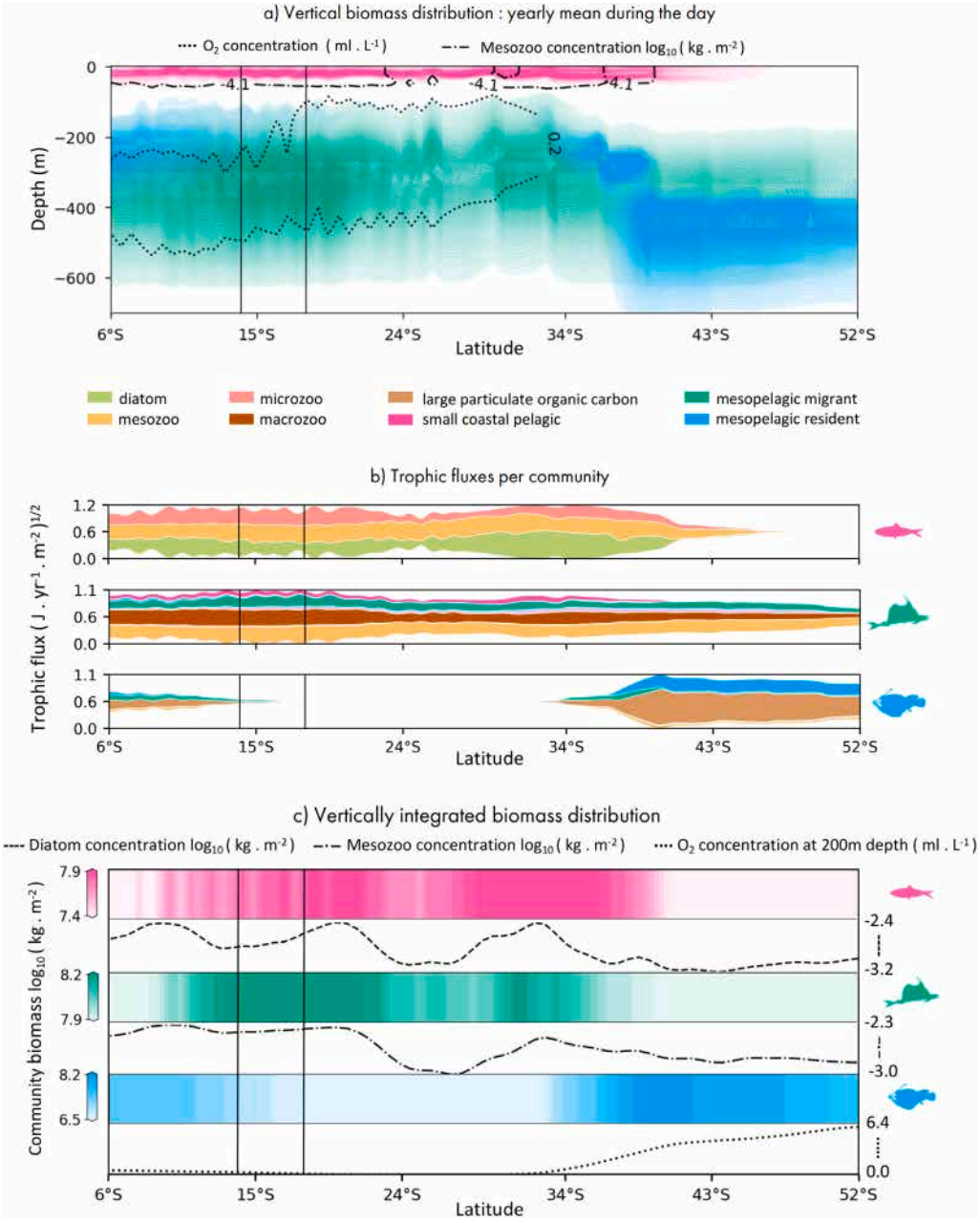

Fig. 3. Distribution and diet of small coastal pelagic and mesopelagic communities in the Humboldt Current System region. (a) Transect along the Humboldt Current System showing the vertical distribution of each APECOSM community from the surface to 700 m depth. Temperature and oxygen limits are shown as isolines. (b) represents the square root of the trophic fluxes (the total flux of energy eaten by a community in $J.yr^{-1}m^{-2}$) and the average diet (i.e. the proportion of each prey component) for small coastal pelagic and mesopelagic communities along the Humboldt Current System transect. (c) represents the biomass distribution of the small coastal pelagic, mesopelagic migrant and resident along the transect, in relation to average oxygen concentration at 200 m and low trophic levels abundance. All figures in the panel represent 2000–2020 averages.

pathways, and re-oxygenating during nocturnal ascent to high-oxygen surface waters (Seibel, 2011; Childress and Seibel, 1998; Urmy et al., 2012). The model captures this diel vertical migration pattern, simulating a shallower vertical distribution of this community in the OMZ region (Fig. 3a), and night-time feeding on surface zooplankton and small pelagics (Fig. 3b). This behaviour confers an ecological advantage to mesopelagic migrants in OMZs by providing refuge from large visual predators with higher oxygen requirements (Seibel, 2011). The OMZ may also enhance their predation efficiency by aggregating their prey in the oxygenated surface layers (Wishner et al., 1998).

Consistent with the model results, acoustic and trawl surveys confirm the presence of important mesopelagic migratory biomass within the OMZ (Cornejo and Koppelmann, 2006; Antezana, 2009), albeit with reduced species diversity (Gjosaeter, 1984) and behavioural adaptations such as earlier diel ascent and reduced activity to minimise metabolic costs (Farquhar, 1971).

In contrast, the distribution of mesopelagic resident organisms is more fragmented in our simulation. They occupy shallower depths from 6 °S to 15 °S, avoiding the OMZ core, and are virtually absent between 15 °S and 31 °S, where the OMZ is at its shallowest. South of this zone, their biomass increases and their vertical distribution deepens, ranging from 400 to 600 m. This community is therefore significantly impacted by the OMZ, with dramatically reduced biomass in the core of the OMZ and shallower vertical ranges in its periphery. Field observations support this result as acoustic profiles show only a weak nocturnal signal

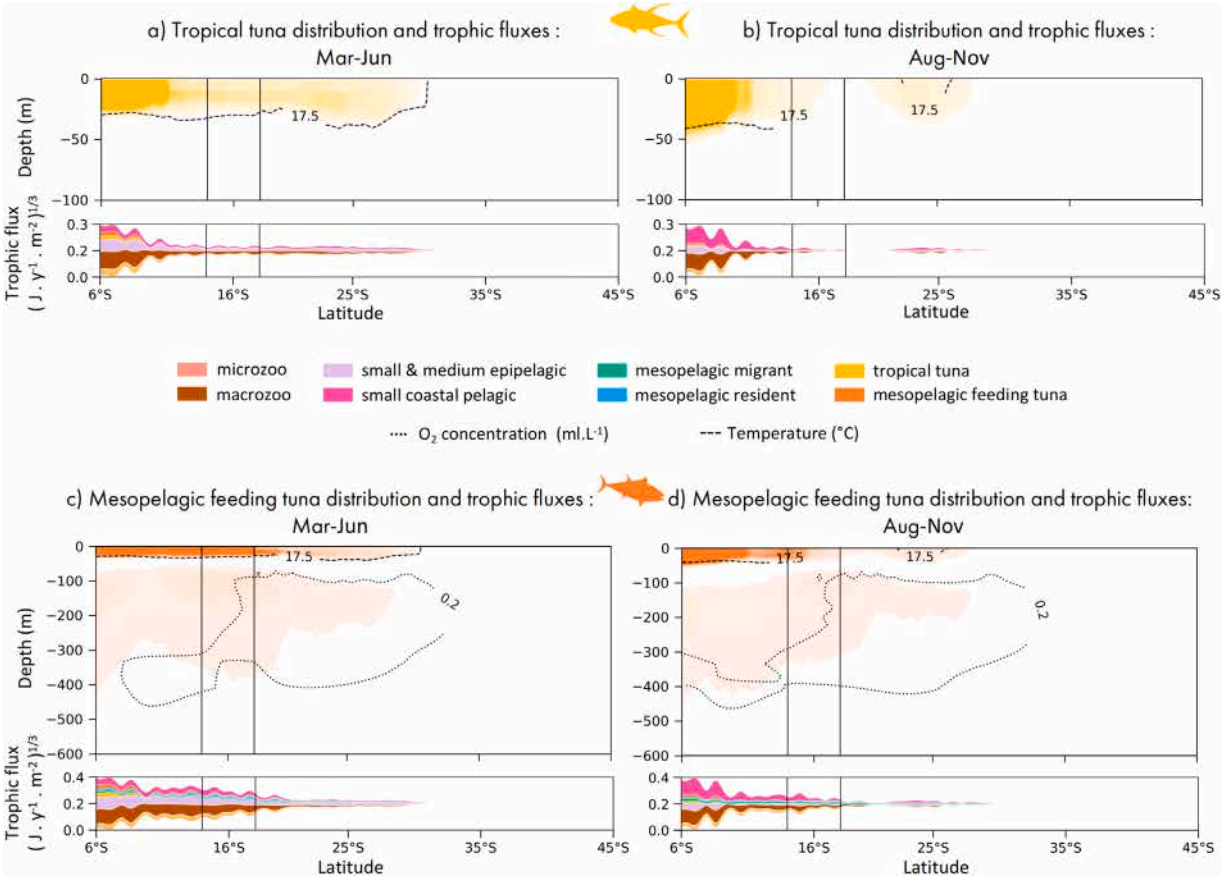

Fig. 4. Tuna distribution, trophic fluxes and diet in the Humboldt Current System. (a) and (b) show the vertical distribution of the tropical tuna biomass along the transect from 6 to 40 °S during 2 periods : from March to June (warm period) and from August to November (cold period). (c) and (d) show the vertical distribution of the mesopelagic-feeding tuna biomass along the transect from 6 to 40 °S during the same periods. Oxygen and temperature limitations are overlaid on vertical distributions. The cubic root of the size- and depth-integrated trophic fluxes (the total flux of energy eaten by a community in ($J.yr^{-1}m^{-2}$)) and diet (relative proportion of each prey component) are shown below along the Humboldt Current System transect, for both communities.

of mesopelagic residents in Peruvian waters (Cornejo and Koppelmann, 2006). Further south, in regions of higher oxygen levels like central and southern Chile, simulated biomass increases significantly. This pattern reflects the metabolic limitation imposed by the OMZ, which inhibits energy-intensive activities such as locomotion and foraging (Seibel, 2011), and can ultimately prevent even basal metabolism in the most deoxygenated waters. In addition, the OMZ significantly reduces the abundance of zooplankton, limiting prey availability to a few hypoxia-tolerant species that exhibit sluggish behaviour (Soviadan et al., 2022). This leads to overall lower biological activity in the OMZ, which in turn decreases the fragmentation of particulate organic carbon (POC). The resulting faster sinking and lower remineralisation rates reduce food availability for mesopelagic residents (Cavan et al., 2017). This is visible in the diet of the mesopelagic residents (Fig. 3b), which are important consumers of POC (e.g. see Dalaut et al. 2025). These limitations further exacerbate the survival challenges of this community in the OMZ region.

3.1.5. The seasonal movements of tunas

In our simulation, the tropical tuna community and the mesopelagic-feeding tuna community have strong thermal preferences, avoiding waters below 18 °C and 15 °C, respectively. Fig. 4 shows their vertical distribution, trophic flux and diet along the HCS transect for two key seasonal periods: the warm season (4a and c), and the cold season (4b and d). Tropical tunas and juvenile mesopelagic-feeding tunas are distributed in the upper 50 m of the water column along the Peruvian coast, while large mesopelagic-feeding tuna individuals dive as deep as 500 m during the daytime to forage on mesopelagic prey. The modelled horizontal distribution of tunas varies seasonally, revealing two distinct patterns. During the warm season (March to June, Fig. 4a and c), tropical tunas extend southward to 28 °S and mesopelagic feeding tunas to nearly 29 °S. The latitudinal distribution of tunas in the model is not primarily constrained by prey availability, since macrozooplankton and small epipelagic communities remain abundant beyond the southern limit of tuna presence, but rather by temperature constraints. Tuna only extend southward during the warmer months, remaining in waters above 17.5 °C. This thermal limitation explains the localised presence of tuna around 24 °S during the cold season (August to November, see the isotherm Fig. 4b and d), likely entering from offshore warm waters rather than migrating along the coast, or being trapped in localised warm-water pocket. The seasonal movements simulated by APECOSM are consistent with observations of the seasonal fishing of skipjack and yellowfin tuna off the coasts of southern Peru and northern Chile (Fink, 1970; Fuller et al., 2021; IATTC, 2022). In northern Peru, seasonal temperature changes have limited effects on the distribution of tuna in the model, consistently with the year-round fishing of yellowfin and skipjack tuna in this region (Broadhead, 1964).

During the warm season, the trophic fluxes generated by the two tropical and mesopelagic-feeding tuna groups indicate that they forage actively north of 28 °S and 29 °S, respectively (Fig. 4.a and c). They forage on the high prey concentrations in the core of the upwelling, where the shallow oxycline enhances prey availability and schooling near the surface (see Supplementary Material 11a). The HCS is well-known for supporting abundant forage species such as the red squat lobster *Pleuroncodes planipes* (Yapur-Pancorvo et al., 2023; Fuller et al., 2021), krill *Nyctiphanes simplex*, and the Peruvian anchoveta *Engraulis*

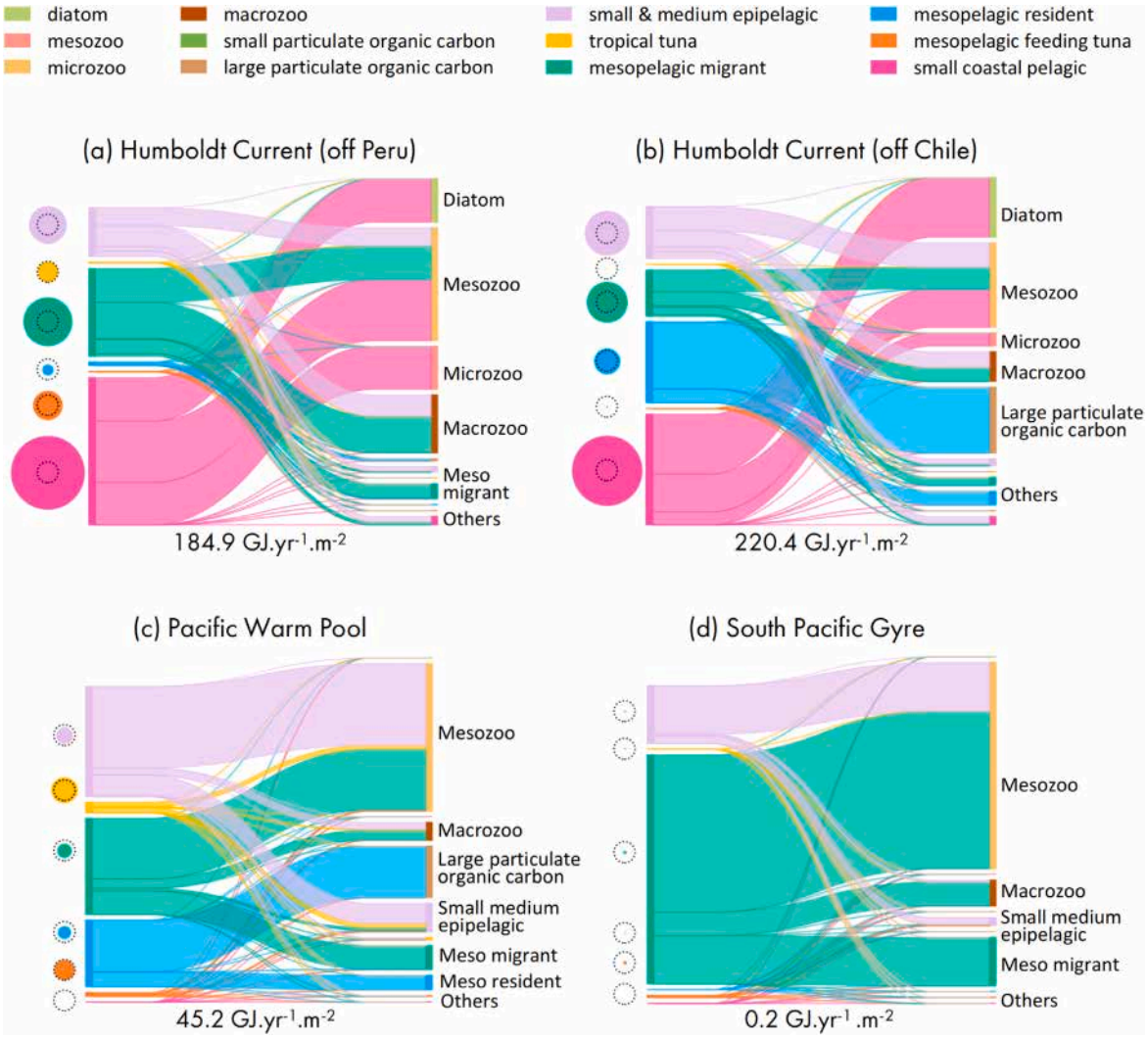

Fig. 5. Trophic fluxes. Trophic fluxes simulated by APECOSM in the northern (a) and southern (b) Humboldt Current System, the Pacific Warm Pool (c), and the South Pacific Gyre (d). The full circles to the left of the Sankey plots represent the regional biomass densities of the six APECOSM communities relative to their global averages (dashed circles). The left axis of each Sankey plot shows predation-driven energy fluxes, with the width of the connectors proportional to the energy flux ($J.yr^{-1}$) and colour-coded by predator group. The right-hand axis shows the trophic source groups from APECOSM and PISCES. The value below each Sankey plot corresponds to the total regional energy flux to HTLs ($GJ.yr^{-1}$), averaged over 2000–2020.

ringens (Fuller et al., 2021). Simulated diets during this season are dominated by small fish, including small coastal and small to medium epipelagics, as well as meso- and macro-zooplankton (Fig. 4a and c). Large mesopelagic-feeding tunas additionally consume mesopelagic migrants and residents. The trophic fluxes and diet shown in Fig. 4 represent values integrated across all sizes (size-explicit diets are shown Fig. 10 in Supplementary Materials; they show the dietary shift towards mesopelagic prey when mesopelagic-feeding tuna start hunting in deep waters). They are therefore weighted towards the diet of the most abundant size classes. Large, deep-feeding tuna are less limited by temperature, however, the intense and shallow OMZ does not enable them to forage efficiently in deep waters beyond 17 °S. During the cold season (August to November, Fig. 4c and d), both tropical and mesopelagic-feeding tuna distributions contract northward, and do not extend beyond 18 °S and 20 °S respectively, with a localised presence around 22 °S to 28 °S. South of 16 °S and 17 °S, trophic fluxes drop sharply, with only a narrow band of foraging activity persisting near 25 °S.

3.1.6. A rich trophic network

Predator–prey interactions are key drivers of marine ecosystem dynamics and major determinants of energy flow within trophic networks (Belgrano et al., 2005). This section examines the trophic energy fluxes simulated by APECOSM in the HCS, from LTL and HTL prey to HTL predators (Fig. 5a and b, Supplementary material 12a and b).

As discussed in Section 3.1.2, small organisms and plankton-feeding small coastal pelagics dominate the total community biomass, leading to trophic fluxes largely driven by lower trophic levels (Fig. 5). The productive HCS supports a variety of HTL communities, with all six simulated groups present off the coast of Peru. Only tropical tunas and mesopelagic resident communities do not exhibit biomass above the global average in the north (Fig. 5a and b left circles).

In the northern HCS, trophic fluxes are dominated by the consumption of small coastal pelagics. This is the only HTL community to feed on diatoms and microzooplankton, while mesozooplankton support a broader set of communities, including small and medium epipelagics and mesopelagic migrants. Macrozooplankton provide energy for mesopelagic migrants, small and medium epipelagics, and,

to a lesser extent, for tunas. Large POC fluxes to mesopelagic residents in significant in the South, while they are scarce in the north. Consequently, the energy flux directed towards small coastal pelagics appears to be lower in the south, but, the differences in absolute values compared to the north are not significant. Both subregions display densely connected size-disaggregated trophic networks, with 3437 and 3439 trophic links respectively across 100 size classes, 6 LTL groups and 6 HTL communities (see Supplementary Material 12).

The shallow oxycline in the north enhances predator efficiency by concentrating prey into surface layers, where they form dense swarms and schools vulnerable to predation (Bertrand et al., 2008b) (Supplementary Fig. 11). High LTL biomass and aggregation support the dominance of small coastal pelagics, which account for 51% of the HTL-directed trophic fluxes in this region. In contrast, the deeper oxycline in the south allows for a greater presence of mesopelagic residents, which feed on sinking POC and on each other. The trophic fluxes to tunas are weak in the north due to their relatively small biomass compared to that of the region's dominant groups. They are even weaker in the south where tunas are largely absent due to colder waters.

The HCS sustains an energetically rich trophic web, with intense transfers across communities and size classes. The model simulates a total annual trophic flux of 184.9 and 220.4 $GJ.yr^{-1}$ m^{-2} in the northern and southern subregions, respectively. Direct LTL–HTL interactions dominate in the region, representing 88.4% of total fluxes (although we overlook the importance of warm-blooded top predators here).

Trophic fluxes from the epipelagic to the mesopelagic organisms are also significant, comprising 31.7% of total energy transfers in the HCS. In the north, mesopelagic migrants contribute 25.4% of total fluxes by feeding in surface waters. In the south, vertical fluxes (36.4%) result from the recycling of large organic particles consumed by mesopelagic residents. This process is inhibited in the north by the shallow and intense OMZ (Fig. 5a and b).

Overall, the HCS exhibits the highest average trophic fluxes among the three regions considered, underpinned by strong LTL–HTL coupling and vertical connectivity across the water column. Passive transport of HTL biomass out of the HCS by Ekman-driven westwards flowing currents and by the northwards flowing bifurcation of the South Pacific Current affects all the communities (see Supplementary Material 13a). With this strong export, the region behaves as an ecological 'source', which continuously fuels neighbouring regions such as the SPG, which acts as a 'sink' (see below 3.3.5).

3.2. The Pacific Warm Pool

In contrast to the cold and productive HCS, the PWP supports high biomasses of large epipelagic predators such as tropical tunas, despite its relatively oligotrophic characteristics. In this section, we first describe the physical and biogeochemical characteristics of the region (Section 3.2.1). We then analyse the region's community size spectrum (Section 3.2.2). Next, we address the paradox of how this nutrient-poor environment sustains dense top predator populations (Section 3.2.3), and explore the role of bathymetry and seamounts in shaping community structure and behaviour (Section 3.2.4).

3.2.1. The Pacific Warm Pool: a warm, stratified, and low-nutrient zone

The PWP, which extends from 100° E to 160° W (Fig. 1), is unique for its particular hydrology. The accumulation of warm surface water deepens the thermocline and drives intense atmospheric convection, influencing the climate over the entire Indo-Pacific region and beyond. The climate in this region is seasonally modulated by the monsoon system, with dominant wind directions reversing between the dry (late June to late September) and wet (December to March) seasons. The ocean in this equatorial region is weakly stratified, with warm sea surface temperatures above 28 °C throughout the year (De Deckker, 2016). Limited by a lack of dissolved iron, phytoplankton productivity is relatively low (Fiedler and Lavín, 2017). This low level of productivity contrasts sharply with the region's extremely high fisheries yields, particularly for tropical tuna. This raises questions about the mechanisms that sustain such high concentrations of top predators in the region.

3.2.2. Stable size spectra and top predator dominance

Modelled size spectra in the PWP (Fig. 2c) reveal higher biomass levels in tropical tunas and mesopelagic-feeding tunas than in the other regions. In contrast, small coastal pelagics are absent, consistent with their preference for cooler waters (Dalaut et al., 2025) and supported by empirical observations (Checkley et al., 2017).

Mesopelagic communities composition show a crossover: the resident community dominates up to 10 g (8 cm), size beyond which the migratory community becomes more abundant. This shift may be due to the shallower bathymetry of the western PWP, which limits suitable habitat for the large resident organisms that typically forage in deeper layers (Dalaut et al., 2025), thereby reducing their abundance and predation pressure on smaller migratory prey.

Unlike the HCS, the PWP exhibits remarkably stable size spectra throughout the year (Fig. 2c), reflecting the low environmental seasonality of the equatorial region (De Deckker, 2016), where interannual variability plays a more dominant role (Barrier et al., 2023).

3.2.3. High HTL biomass in an oligotrophic region?

Fig. 6 presents vertical distribution of mesopelagic (Fig. 6a) and tunas (Fig. 6b) communities, the main environmental drivers (Fig. 6c, d, e), schooling probability (Fig. 6f), trophic fluxes and diets (Fig. 6g) for the four APECOSM communities that we emphasise in this region : the two tuna communities and the two mesopelagic communities. Fig. 1a shows that total HTL biomass exhibits pronounced meridional and zonal gradients, with a higher concentration of biomass near the equator and a decrease in biomass to the west along the transect. This zonal gradient divides the region into two ecological subzones.

The western part of the region (130–170 °E; region A) is characterised by a deep thermocline and warm waters accumulating at the surface with the 29 °C isotherm extending to 50 m depth (Fig. 6d). This region experiences limited nutrient inputs from both vertical and horizontal processes (Radenac et al., 2013), resulting in reduced primary production and lower HTL biomass. The deep and diffuse thermocline concentrates both epipelagic (daytime) and mesopelagic migrant (nighttime) communities around 100 m depth, where temperatures remain suitable for tropical tunas and light levels sufficient for visual predation (Fig. 6c, d). Mesozooplankton biomass peaks in the western part of the subregion (Fig. 6c), with tunas constrained above 100 m due to light limitations. Mesopelagic migrants feed nocturnally in this layer, following prey distributions. A notable aggregation peak occurs around 138° E (Fig. 6f), coinciding with shallower seafloor, where mesopelagic migrants constitute a significant proportion of tuna diet and intra-community predation (Fig. 6g). Topical tunas show intensive schooling around 160° E, where they are concentrated vertically by deeper food sources pulling them down, and by light constraints pulling them up. In contrast, mesopelagic residents are sparse in the eastern subregion, limited by the reduced availability of POC (Fig. 6e).

The favourable conditions enable broader vertical distributions of HTL communities, with mesopelagic-feeding tunas exhibiting size-dependent depth preferences : small individuals in shallower layers and larger individuals deeper, co-occurring with abundant mesopelagic residents. Both tunas and mesopelagic migrants track mesozooplankton, which is deep in this region, resulting in expanded vertical distributions. Schooling behaviour is generally enhanced in this region, despite mesopelagic migrants' schooling rates overshadowed by the sharp aggregation peak at 138 °E (Fig. 6f). Other HTL groups also school more actively in Region B (Fig. 6c), particularly in areas with higher productivity. Diet compositions reflect local prey availability,

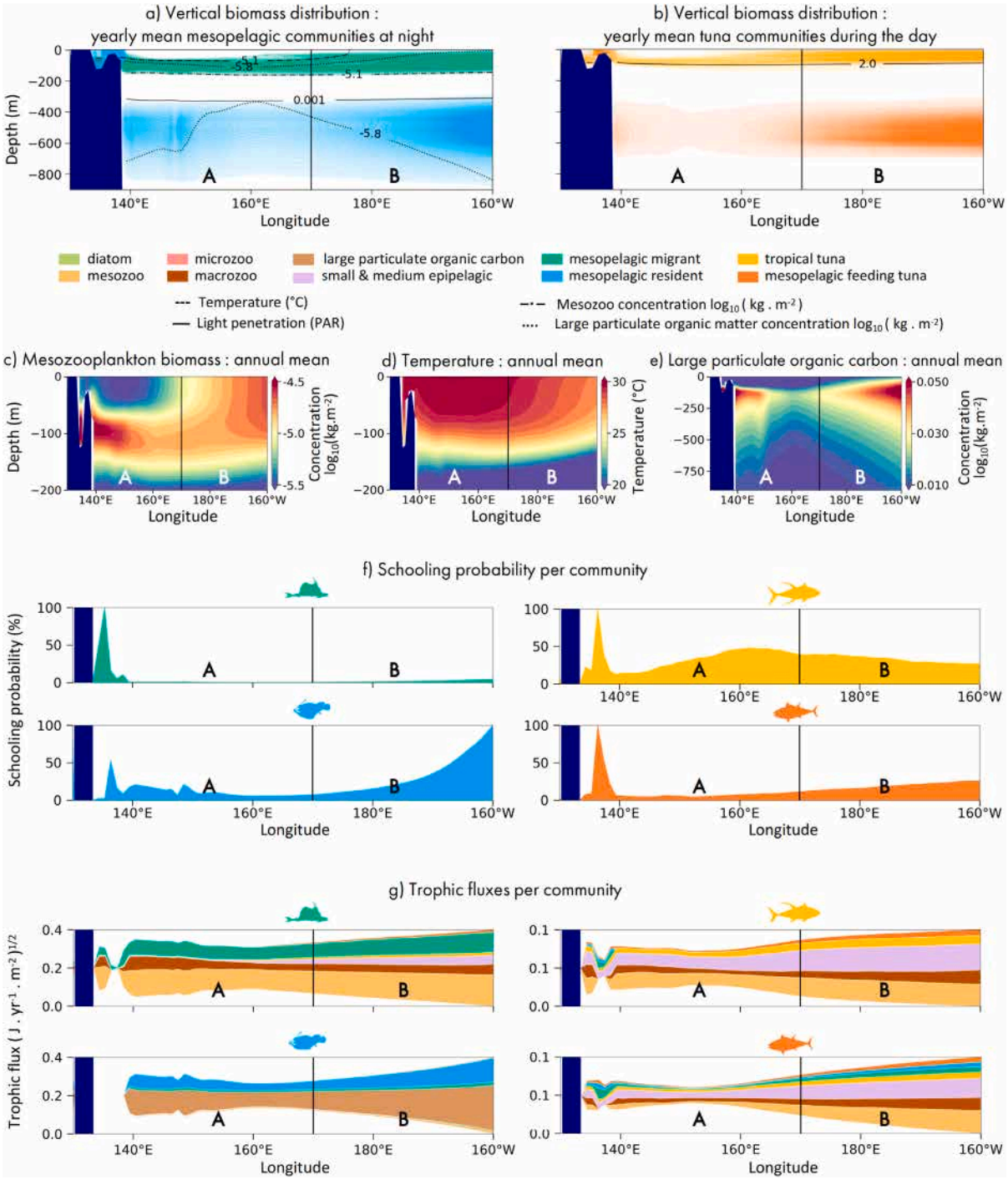

Fig. 6. Pacific Warm Pool analysis. Vertical distribution of total biomass averaged over 2000–2020 is shown for (a) mesopelagic communities at night and (b) tuna communities during the day. Subregions A and B highlight distinct physical and biogeochemical characteristics, detailed in panels (c–e): (c) mesozooplankton concentration, (d) temperature profiles, and (e) large particulate organic carbon (POC) concentrations. Panel (f) displays schooling probability, while (g) presents the square root of the trophic fluxes and diet composition of tuna and mesopelagic communities along the transect, averaged over 2000–2020.

with tunas consuming primarily small and medium epipelagics, mesozooplankton, and macrozooplankton, while mesopelagic-feeding tunas incorporate mesopelagic communities in their diet, particularly in large size classes (see Supplementary Material 10). Mesopelagic residents mainly consume POC and smaller members of their own community.

The increased biomass of HTL communities observed in region B (Fig. 6a,e,f) is largely due to passive biomass transport from the productive Cold Tongue region through zonal advection by the equatorial current. This biomass transport affects particularly the small and medium epipelagic community as well as the two tuna communities (see supplementary Material 14a), which also likely concentrate actively in this warm and prey-rich region where they feed and reproduce. Thanks to this strong biomass import, the region behaves as an ecological 'hub' fuelled by the Cold Tongue 'source', and evacuating biomass

both sides of the equator to the northward flowing Kuroshio current and the southward flowing East Australian Current (see Supplementary Material 14b). Overall, the net biomass import/export flux in the region fluctuates around zero for the small and medium pelagics, while it is clearly positive for tunas and mesopelagic residents and negative for migrants (see Supplementary Material 13b and 14). This shows that small and medium epipelagics enter the region passively through its eastern boundary and are exported northwards and southwards. In contrast, tunas, which are also imported from the east, actively swim towards the equator to remain in the region, where they concentrate. This underscores the open system nature of regional ecosystems, which are strongly influenced by neighbouring regions through passive biomass transport by oceanic currents and active movements. This also demonstrates that without the influx of small and medium-sized epipelagic prey, the passive entry of tuna and their active retention in the region, such high concentrations of tuna would be unsustainable.

3.2.4. Seamounts influence the vertical distribution, density and trophic interactions of HTLs

The productivity of the westernmost part of the PWP is strongly influenced by its unique topography, characterised by a shallow bathymetry and the presence of seamounts, defined as prominent elevations of the seafloor. Where seamount summits extend into the mixed layer and photic zone, the simulated epipelagic communities are passively concentrated over these features by marine currents, and they exhibit shallower vertical distributions than in surrounding waters (Fig. 6d). However, when we consider the entire water column, they are not more abundant than elsewhere in the transect. Seamounts are known to promote upwelling and mixing (Rogers, 2018; Mashayek et al., 2024), enriching the upper layers with nutrients, and consequently increase the amount of plankton (Fig. 6c). Seamounts also play an important role in global fisheries by acting as aggregation sites for commercially important large pelagic species, including tunas (Fonteneau, 1991; Holland and Grubbs, 2007; Dubroca et al., 2014; Borland et al., 2021). The greater aggregation (Fig. 6h) and shallower vertical distribution of the biomass simulated in APECOSM over seamounts (Fig. 6d) could explain the increased accessibility of these fish to fisheries in these areas. Two main hypotheses have been proposed to explain the elevated densities of tuna and other pelagic species observed around certain seamounts. The first suggests that seamounts act as navigational waypoints within broader migration patterns (Klimley, 1993; Holland et al., 1999; Klimley et al., 2003). However, this behavioural mechanism is not represented in APECOSM. The second proposes that seamounts increase foraging opportunities for apex predators by concentrating their prey through vertical migration, advection, or trapping (Rogers, 2018; Parin et al., 1997; Fock et al., 2002; Musyl et al., 2003). This last hypothesis is consistent with increased HTL schooling over the seamounts, and with the simulated tuna diet in the PWP (Fig. 6i), which includes a notable contribution of mesopelagic organisms, despite tropical tunas and small mesopelagic-feeding tuna foraging mostly in the enlighten epipelagic zone.

Simulated mesopelagic organisms are indeed present over the seamounts (Fig. 6a), a pattern consistent with field observations. Studies have reported a reduction in the species richness and diversity of mesopelagic fish over seamounts compared to adjacent deep ocean waters (Pusch et al., 2004; Annasawmy et al., 2019). Some studies suggest that certain mesopelagic species are seamount-associated, occurring either exclusively or at higher abundances in these habitats (Parin and Prut'ko, 1985; Boehlert and Genin, 1987; Moore et al., 2003). This association of certain mesopelagic species with seamounts is thought to be driven by increased food availability due to localised nutrient upwelling and increased primary production (Pusch et al., 2004). However, these processes are not explicitly resolved in the numerical models used here (NEMO, PISCES and APECOSM), due to their coarse spatial resolution.

3.2.5. Moderate trophic fluxes in the region

All HTL communities are present in the PWP, except small coastal pelagics, which are excluded by high temperatures. Biomasses of small and medium epipelagics and mesopelagic migrants are slightly below average, but still significant despite the low primary production. This is partly due to advective transport from the productive Cold Tongue region, which helps sustain epipelagic foodwebs in the PWP. Tropical and mesopelagic-feeding tunas show average to above-average levels (Fig. 5c). Despite relatively low primary production (see Section 3.1.2), mesozooplankton dominate energy transfers, supporting a wide range of epipelagic feeders, including small and medium epipelagics, mesopelagic migrants, tropical tunas, and juvenile mesopelagic-feeding tunas. A secondary but notable flux arises from large POC, which sustains mesopelagic residents.

Although smaller in magnitude, other fluxes are diverse, highlighting the opportunistic feeding strategies of pelagic predators. Compared to the HCS, the PWP shows an absence of diatom-based fluxes and a limited role for macrozooplankton. The size-structured trophic network consists of 3,036 links, 12% fewer than in the HCS (see Supplementary Material 12).

Mesopelagic communities occasionally occupy epipelagic layers, particularly above seamounts, where they become accessible to tropical tunas. In the eastern part of the PWP, mesopelagic-feeding tunas exploit mesopelagic prey in deeper layers, generating strong trophic fluxes in areas of high tuna abundance (Fig. 6g).

Overall, trophic fluxes remain relatively weak (45.2 $GJ.yr^{-1}m^{-2}$) and diffuse, likely due to limited vertical stratification that hinders prey aggregation. Direct LTL–HTL fluxes account for 75.5% of total energy transfers, lower than in the HCS, while vertical fluxes from surface to deep layers are relatively high (43.2%), largely driven by the recycling of sinking organic particles by mesopelagic residents. Intra-community interactions, particularly within mesopelagic communities, also contribute significantly (13.1%).

3.3. The South Pacific Gyre

The SPG, often described as a marine biological desert, is the least studied of the major subtropical gyres, primarily due to its vast size and geographic remoteness. Existing research has largely focused on its physical and biogeochemical processes, as well as plastic pollution (e.g. Reid, 1986, Halm et al., 2012, Eriksen et al., 2013). In contrast, the structure and dynamics of HTLs in this region remain poorly understood. In this section, we first describe the SPG's physical and biogeochemical characteristics (Section 3.3.1), then we assess how these characteristics shape the regional ecosystem size spectra (Section 3.3.2). Next, we examine how the pelagic HTL communities change across the transition from the East Australian Current (EAC) to the core of the gyre (Section 3.3.3), and explore the trophic interactions and mechanisms governing trophic control within the gyre (Section 3.3.4). Finally, we conclude our analysis of the modelled SPG ecosystem by examining the structure of the trophic network and the 'sink' nature of the HTL communities in the region, which would not persist without continuous biomass import (Section 3.3.5).

3.3.1. The South Pacific gyre: an oligotrophic zone

The SPG, the largest of all oceanic gyres, covers almost 10% of the global ocean surface (Longhurst et al., 1995). It is the defining feature of the oligotrophic South Pacific, formed through the interaction of tropical and subtropical wind systems and the Coriolis effect, which generates an anticyclonic circulation composed of the westward Equatorial Current, the poleward East Australian Current, the eastward mid-latitude South Pacific Current and the eastern boundary Humboldt Current (Roemmich et al., 2016). Despite intense solar irradiance, the downwelling associated with this anticyclonic circulation suppresses vertical nutrient transport to the surface layers, resulting in extremely low nutrient and chlorophyll concentrations, and leading to weak vertical export fluxes of particulate organic matter (POM). As a consequence, primary production in the oligotrophic SPG is weak and mostly

due to small nitrogen-fixing phytoplankton (Halm et al., 2012).

3.3.2. Epipelagic biomass depletion and dominance of the mesopelagic migrants in the size spectra

In the oligotrophic SPG, community size spectra are greatly reduced compared to global averages (Fig. 2d). Small coastal pelagics are virtually absent, and biomass of tropical tunas and small mesopelagic-feeding tunas is also low. Notably, there is an inversion in the relative abundance of mesopelagic migrants and residents : although migrant biomass is two orders of magnitude below the global average, it remains nearly ten times higher than that of residents. The latter are reduced to levels similar to the highly depleted small and medium epipelagic community. The size spectrum of the small and medium epipelagic community exhibits pronounced domes that are stable over time. This pattern may indicate top-down control of these low-biomass communities (Rossberg et al., 2019), and is discussed further in Section 3.3.5. Seasonal variability in the SPG is limited but notable within intermediate-size epipelagic communities (Fig. 2d). This may be driven by seasonal shifts in prey availability or biomass import linked to the seasonal displacement of the gyre system (Barnett, 1983; Schneider et al., 2007; Roemmich et al., 2016).

3.3.3. The ecotone from a rich and productive region to a biological desert

Fig. 7 presents the model outputs along an extended transect crossing the SPG, from the Australian coast to the Chilean coast. Panel 7a shows the vertical distribution of biomass, panel 7b illustrates trophic fluxes, and panel 7c displays size-abundance distributions (i.e. size spectra) as a function of longitude. Together, these elements reveal stark contrasts in absolute and relative biomass, size structure, and vertical distribution of pelagic communities within the gyre (140 °W to 90 °W) compared to adjacent regions to the west and east. The core of the SPG is characterised by very low overall biomass, with a near-total absence of mesopelagic residents, tropical tunas, and small coastal pelagic communities (Fig. 7a). Only limited biomasses of mesopelagic migrants, mesopelagic-feeding tunas, and small and medium epipelagic organisms persist. The longitudinal distribution of these groups mirrors that of mesozooplankton, the primary food source for the small HTL organisms in the region (see isoline Fig. 7a). Among all communities, mesopelagic migrants and mesopelagic-feeding tunas are the most resilient. However, their biomass in the SPG represents only 2.6% and 4.2%, respectively, of that observed outside it, on both sides along the extended transect. Other HTL communities show even lower relative densities, falling below 2% of their level outside the SPG.

These spatial patterns can be understood in light of regional oceanographic processes and species distributions. The SPG is bounded by the EAC to the west and the HCS to the east. The EAC is a dynamic system, featuring mesoscale eddies formed along the Australian shelf and around seamounts. These features enhance vertical mixing and nutrient availability (Ridgway and Hill, 2009), supporting high primary production and a diverse epipelagic fauna including sardine, blue mackerel, jack mackerel, and redbait (AFMA, 2022), as well as mesopelagic migrants, notably the myctophid *Ceratoscopelus warmingii* (Young et al., 2011). In addition, the EAC transports warm tropical waters southward (Ridgway and Dunn, 2003), facilitating the presence of apex predators such as yellowfin tuna (*Thunnus albacares*), striped marlin (*Tetrapturus audax*), bigeye tuna (*Thunnus obesus*), and swordfish (*Xiphias gladius*) (Young et al., 2011). The distribution of these species aligns with the modelled epipelagic communities between 160 °E and 140 °W (Fig. 7b).

Although these species extend eastward, their abundance declines sharply at the entrance to the gyre. Bigeye tuna and swordfish, implicitly part of the mesopelagic-feeding tuna community in the model, extend further east than yellowfin tuna (Young et al., 2011). This pattern is explained in the model by a shift in prey availability: plankton occurs at depths beyond the visual foraging range of tropical tunas such as yellowfin (Fig. 7a, left panel). In the central gyre near the Pitcairn Islands, industrial fisheries are largely absent due to the low abundance and scattered distribution of target species such as tuna (Langley and Adams, 2005).

Beyond total biomass, the vertical distribution of communities also differs markedly. Outside the gyre, epipelagic communities inhabit relatively shallow waters, but their distribution progressively deepens towards the gyre's core. Mesopelagic migrants also shift deeper within the gyre, both day and night (see Fig. 7a and b for the day, night is not shown). Mainly smaller individuals that remain in upper layers are still present in the SPG (Fig. 7c left panel), explaining the absence of migrants below 450 m between 120 °W and 100 °W. On the SPG's western flank, sparse planktonic biomass is further reduced by reduced vertical mixing, enhanced stratification and deep thermocline, contributing to declining HTL biomass. In the model, this reduction in LTL biomass translates into a reduction in HTLs. The progressive deepening of HTL biomass in the SPG reflects both the deepening of LTLs, driven by the presence of a deep chlorophyll maximum (Cornec et al., 2021; Dai et al., 2023), and the increased light penetration in these clear oligotrophic waters.

Observations in the EAC report a deep sound scattering layer around 500–600 m, corresponding to mesopelagic residents (Young et al., 2011), consistent with APECOSM outputs (Fig. 7b). This community is particularly sensitive to reduced primary production, which leads to low POM export. In the model, decreased LTL biomass lowers the vertical flux of POM, a key food source for mesopelagic residents (Dalaut et al., 2025). Additionally, the SPG's food web is dominated by small picoplankton and heterotrophic bacteria (Claustre et al., 2008), which transform POM into dissolved organic forms (Kong et al., 2021), further reducing its availability for deep-sea consumers. Consequently, mesopelagic residents experience severe food limitation in the gyre.

Distinct community compositions emerge on the eastern and western flanks of the SPG. To the west, the warm waters of the EAC prevent small coastal pelagics, which are associated with cold-water, from inhabiting the area. To the east, the cold, nutrient-rich HCS limits the presence of tropical tunas and mesopelagic-feeding tunas. Moreover, the OMZ in the eastern flank compresses the vertical habitat of both epipelagic and mesopelagic communities, pushing their distributions upward and substantially reducing mesopelagic resident biomass (see Section 3.1.4).

3.3.4. Trophic interactions control the size distribution of remaining communities

In the SPG, the size spectra of the two more resilient communities (mesopelagic migrants and mesopelagic-feeding tunas) differ markedly from those in adjacent, more productive regions. Within the SPG, mesopelagic migrants exhibit a reduced presence of large individuals compared to surrounding areas (Fig. 7c, left panel). In certain South Pacific zones, particularly around French Polynesia, mesopelagic migrant species are sporadically targeted by fisheries, especially near seamounts or close to the surface at night during full moons. These include deep-sea species such as *Taractichthys steindachneri*, *Eumegistus illustris*, *Taractichthys longipinnis*, and *Brama brama* (Misselis and Ponsonnet, 2015).

In contrast, mesopelagic-feeding tunas within the SPG display a discontinuous size distribution, with individuals primarily in the 5–30 cm range and around 1 m, while both smaller and larger size classes are largely absent (Fig. 7c, right panel). Larger individuals are concentrated along the western transect, while fewer and smaller ones are found on the eastern side. Large pelagic species such as bigeye tuna (*Thunnus obesus*), swordfish (*Xiphias gladius*), and yellowfin tuna (*Thunnus albacares*), which correspond to the mesopelagic-feeding and tropical tuna communities, are rarely caught in the core of the SPG. Although longline fisheries operate in its periphery (Fonteneau, 1997; Allain et al., 2016; Moore et al., 2020; Coghlan et al., 2017), size-specific catch data remain scarce, precluding direct comparisons with APECOSM outputs. Overall, fisheries activity within the SPG remains very limited due

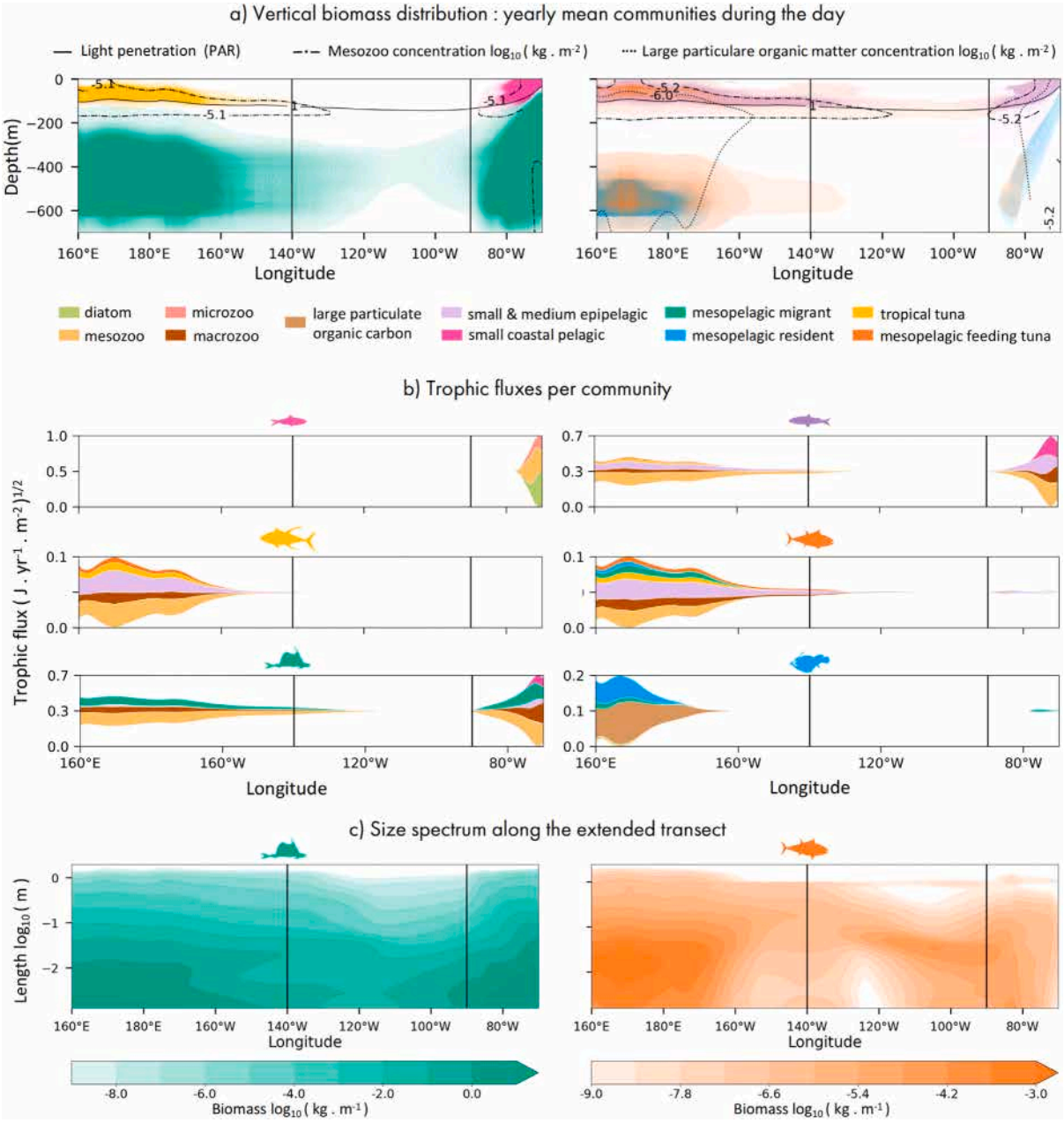

Fig. 7. South Pacific Gyre analysis. (a) represents the yearly mean vertical distribution of communities along the extended transect. Isolines of the main limiting factors are drown for light (continuous), mesozooplankton (dashed), and large particulate organic matter concentration (dotted), with communities split in two plots for improved visibility. The two vertical lines delimit the core of the gyre. (b) shows the square root of the trophic fluxes and diets for each community along the extended transect. (c) represents the size spectra along the extended transect for mesopelagic migrants (left) and mesopelagic-feeding tuna (right) communities. All the figures in this panel represent averages over the 2000–2020 period.

to the scarcity of commercially valuable species and the geographical remoteness (Allain et al., 2016; Moore et al., 2020). Exceptions include some artisanal and industrial longline fisheries (Coghlan et al., 2017; Andréfouët and Adjeroud, 2019; Karcher et al., 2020; Zylich et al., 2014), and fisheries targeting albacore (*Thunnus alalunga*), a species not included in the current APECOSM configuration and typically found in the northern side of the gyre rather than in its core (Moore et al., 2020; FAO, 2011).

In the EAC, the trophic fluxes to the small and medium epipelagic community are primarily supported by mesozooplankton. Large organisms within this community increasingly rely on intra-community predation and macrozooplankton. Tuna communities exhibit similar feeding patterns, with a lower dependence on mesozooplankton, and in the case of mesopelagic-feeding tunas, a notable incorporation of mesopelagic prey. Mesopelagic migrants mainly consume mesozooplankton, with secondary inputs from macrozooplankton and intra-community predation. In contrast, mesopelagic residents rely heavily on POC and mesopelagic organisms, especially from its own community.

Within the SPG, trophic fluxes are drastically reduced. For the size classes that persist in this oligotrophic environment, mesozooplankton remains the dominant prey, indicating a strong dependence of small predators on this limited resource (see Supplementary Material 10d). Contributions from larger prey are minimal and therefore barely discernible in the figure. Mesopelagic-feeding tunas larger than 10 cm predominantly feed on macrozooplankton and small to medium epipelagic fish. Individuals above 30 cm gradually incorporate their own community into their diet. A similar dietary shift occurs among mesopelagic

migrants, which transition from macrozooplankton to intra-community predation beyond 5 cm in length.

In APECOSM, large sized organisms in the SPG are rare across all communities and rely heavily on feeding within their own community. The scarcity of large individuals (Fig. 2d, 7d) likely reflects the imbalance between the low food availability and the high energetic needs of large organisms (Kooijman, 2010). Consequently, tunas inhabiting the SPG are generally smaller than those in more productive regions such as the PWP and the western South Pacific (Fig. 2d), consistently with observations (Moore et al., 2020).

3.3.5. A sparse trophic network relying on intra-community predation and lateral biomass import

The SPG sustains the lowest biomass and diversity among all regions studied, with an average energy flux of only 0.2 $GJ.yr^{-1}.m^{-2}$. Biomass levels across all HTL groups fall far below global averages, especially for small and medium epipelagics, tunas, and mesopelagic migrants. Mesopelagic residents and small coastal pelagics are nearly absent (Fig. 5d).

Energy fluxes are primarily driven by mesozooplankton, which supports small and medium epipelagics and mesopelagic migrants. Migrants exert significant trophic pressure on both macrozooplankton and their own community, mirroring patterns observed for the small and medium pelagic community. Beyond these dominant links, the size-structured trophic network is extremely sparse, with only 2,873 trophic connections, 16% fewer than in the HCS (Supplementary Fig. 12). Trophic fluxes are overwhelmingly dominated by predation from the mesopelagic migrants (79.2%), followed by small and medium epipelagics (20.0%). Mesopelagic-feeding tunas remain rare, contributing just 0.75% of total flux. Despite having higher abundance than mesopelagic-feeding tunas, mesopelagic residents exhibit negligible feeding activity (< 0.0001%) and contribute insignificantly to energy transfer (Fig. 7c; Supplementary Fig. 10d). This likely reflects metabolic adaptations to the deep, cold environment, that enable them to survive for long periods without feeding. In this oligotrophic environment, only few HTL communities are able to persist. Small and medium epipelagics, mesopelagic migrants, and mesopelagic-feeding tunas survive by exploiting all available resources, including their own community. This likely explains the double-domed size spectra (Fig. 2d), which results from strong intra-community predation (Rossberg et al., 2019) and accounts for 19.3% of total trophic fluxes in the SPG.

Overall, the trophic network in the core of the SPG is sparse and weakly connected. The functional responses of HTL communities (the degree of satiation of individuals) are too weak to sustain stable HTL populations (Supplementary Fig. 10). The presence of HTLs in the core of the SPG is therefore likely transient and maintained through continuous passive biomass transport by Ekman-driven centripetal currents from more productive neighbouring regions such as the EAC, the HCS or the Cold Tongue. Thanks to this biomass import that affects all the communities (see Supplementary Material 13c), the region behaves as an ecological 'sink' continuously fuelled by the rich regions surrounding the gyre, which act as 'sources'. Without such import, the region would not sustain HTLs in its core.

4. Discussion-conclusion

4.1. Contrasting trophic transfer and network structure across ecosystems

The structure and functioning of marine food webs vary substantially across oceanic regions, influencing biomass accumulation, energy transfer, and ecological stability. The HCS, PWP, and SPG exemplify three contrasting ecosystems in terms of primary productivity, trophic connectivity, and community structure. By comparing simulated trophic transfer efficiency and food web complexity, we examine how energy flows from low to high trophic levels through trophic networks under different environmental regimes.

A key emerging distinction among the regions is their trophic transfer efficiency, approximated here by the ratio of high- to low-trophic level biomass (HTL/LTL, Fig. 8a). This ratio scales non-linearly with productivity: it is at its lowest in the oligotrophic SPG (0.005), intermediate in the moderately productive PWP (0.130), and at its highest in the highly productive HCS (0.361). These differences reflect not only resource availability, but also the efficiency with which energy is transferred through the food web under different structural configurations and temperature constraints.

The SPG is characterised by inefficient trophic transfer from LTLs to HTLs. In productive systems, diatom-based primary production feeds directly into the mesozooplankton and HTL food chains. In contrast, primary production in the SPG is dominated by small phytoplankton, such as picoplankton and flagellates. These are consumed by microzooplankton, adding an intermediary to the food chain between phytoplankton and mesozooplankton, and increasing energy losses and dissipation (Bi et al., 2021; Young et al., 2011). The SPG can be considered as an ecological 'sink', maintained by the continuous import of biomass from the rich surrounding regions that act as 'sources' by exporting more than they import (see Supplementary Material 13c). In contrast, upwelling systems such as the HCS act as 'sources'. In these highly productive systems, strong nutrient inputs in the euphotic region support the production of large phytoplankton (e.g., diatoms), which is directly consumed by mesozooplankton, thus shortening trophic chains and improving trophic transfer efficiency between LTLs and HTLs (Armengol et al., 2019). The PWP occupies an intermediate position. Despite deep nutricline and weak vertical mixing, nutrients advection from the Cold Tongue allows moderate productivity. Continuous HTL biomass import and predator aggregation lead to surprisingly high HTL biomass levels, turning this region into a rich and diverse ecological 'hub' despite its weak primary production (see Supplementary Materials 13b and 14). Temperature plays an additional regulatory role. In warm regions like the PWP and the SPG, elevated metabolic rates lead to higher energy losses, reducing the proportion of assimilated energy that reaches HTLs (Guiet et al., 2016; Barneche et al., 2021). Consequently, HTL biomass in these regions reflects not just bottom-up limitations and lateral import/export, but also thermodynamic constraints.

The non-linear scaling of HTL biomass relative to LTL biomass (Fig. 8a) also reveals threshold-like dynamics. At low LTL biomass, HTL biomass remains negligible. As the biomass of LTLs increases, HTLs increase disproportionately, but reach a plateau at high LTL biomass, as in the HCS. This apparent saturation suggests that there are diminishing returns for predator biomass beyond a certain level of prey density.

This variability in trophic transfer is also evident in regional size spectra (Fig. 8b). The HCS exhibits size spectra that exceed global averages, driven by the abundance of small coastal pelagics (first dome) and supplemented seasonally by larger transient predators (second dome). By contrast, the PWP exhibits an inverted pattern: the second dome is dominant due to sustained predator accumulation and biomass import, while the first dome is subdued by low LTL productivity. The SPG displays both domes, but at vastly reduced biomass levels. The first dome declines steeply due to the scarcity of small epipelagics, while the second dome, corresponding to large predators, is nearly three orders of magnitude below global average. These patterns emphasise the interaction between bottom-up forcing, lateral import, thermal regimes and size-based predation in shaping size structure across environmental gradients.

Contrasts in trophic transfers are reflected in both the diversity and intensity of trophic interactions. These are measured using a Shannon–Weaver index (H') applied to trophic fluxes, as well as the interaction strength of trophic links (F) (cf. Fig. 9 and Supplementary E for index calculations). The HCS exhibits the most diversified and intense trophic fluxes and interaction strength F, particularly in its southern domain, where values reach $H' = 5.3$ and $F = 0.0568$. This reflects a highly interconnected food web with strong vertical energy transfers from the epipelagic realm to the mesopelagic one, dense trophic coupling across

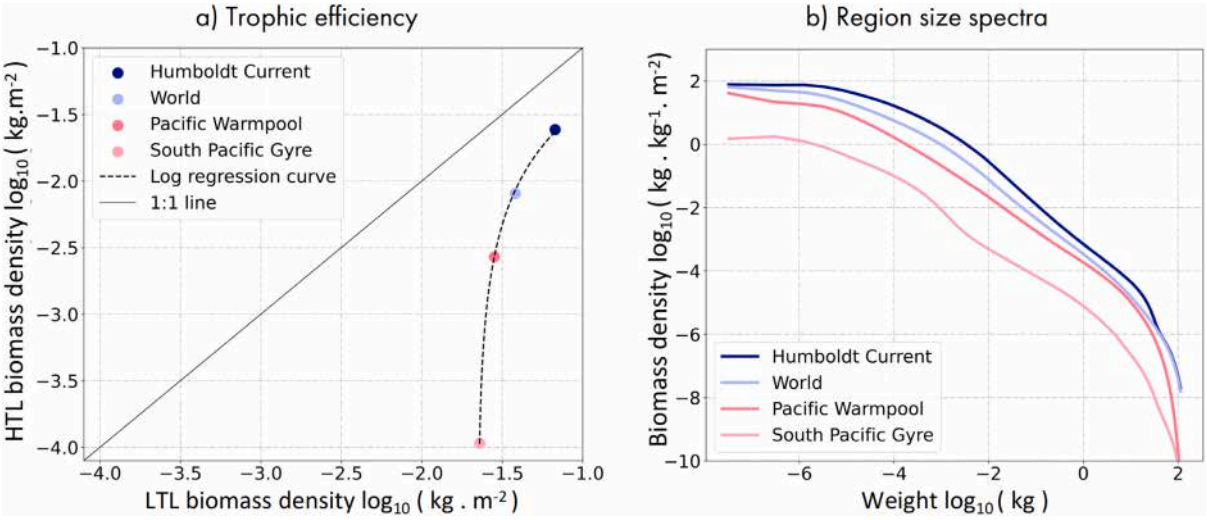

Fig. 8. Trophic efficiency and size spectrum across regions. (a) average biomass density of high trophic levels (all communities) simulated by APECOSM, as a function of the average biomass density of all LTL communities simulated by PISCES in every region. (b) average HTL size spectra (all communities) simulated by APECOSM in every region. Both plots are based on 2000–2020 averages.

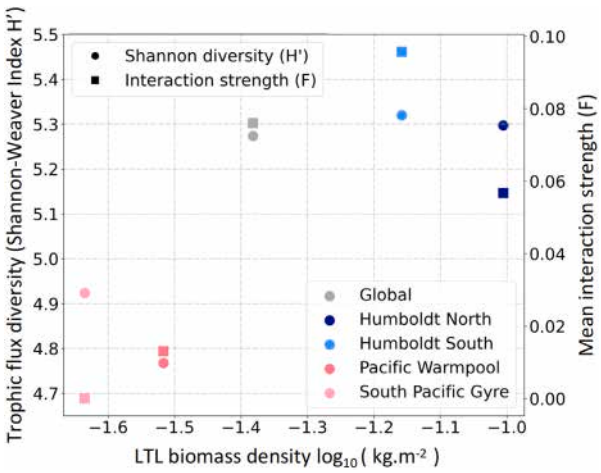

Fig. 9. Flux diversity and strength. Representation of interaction strength F and trophic flux diversity (Shannon–Weaver index H) across the four regions, based on trophic fluxes averaged over the 2000–2020 period in each region and globally.

size classes, and a large number of trophic pathways. The northern HCS exhibits a comparable structure, albeit with weaker interactions, likely due to the inhibitory effects of the OMZ on the mesopelagic resident community.

By contrast, the PWP exhibits the lowest trophic flux diversity ($H' = 4.77$), alongside moderate interaction strength ($F = 0.0131$). This indicates a simpler, more centralised food web, structured around few dominant pathways involving mesozooplankton, mesopelagic communities and highly mobile predators such a tunas. Despite this simplicity, the presence of numerous size-based links still enables moderate trophic connectivity. However, the dominance of a few species and pathways increases the system's susceptibility to external perturbations such as El Niño–Southern Oscillation (ENSO) events (Barrier et al., 2023), which can drastically impact species distribution and food web stability.

Interestingly, the SPG presents a relatively high trophic network diversity ($H' = 4.92$) but negligible interaction strength ($F = 0.00002$). This combination indicates a fragmented and weakly connected food web, sustained primarily through opportunistic feeding and intra-community interactions. The relatively high H' in this context does not imply ecological robustness but rather reflects many low-intensity interactions among scarce organisms in a depauperate system. The region's food web is shaped by bottom-up energy limitation, infrequent predator–prey encounters, and lateral import from surrounding productive zones.

It is essential to note that the ecosystem model used in this study, APECOSM, aggregates numerous species and taxa into broad functional communities. While this approach enables basin-scale ecosystem simulation, it underestimates the actual ecological complexity and taxonomic diversity of pelagic food webs. Therefore, the indices H' and F should be interpreted as conservative approximations of the heterogeneity and intensity of trophic interactions.

4.2. To recap

This study uses the APECOSM model to examine the emerging ecosystem structure and function across three distinct oceanic regions: the productive Humboldt Current System, the Pacific Warm Pool, and the oligotrophic South Pacific Gyre. Despite being configured at global scale, APECOSM successfully reproduces the main regional patterns, demonstrating its ability to capture the diversity of ecosystem responses to contrasting environmental regimes. LTL biomass, comprising phytoplankton, zooplankton and POM, emerges as the primary driver of community presence and abundance. Simulations also highlight the processes through which regional dynamics are influenced by temperature, stratification, oxygen concentration, currents and location relative to other regional systems, as well as the role of topographic features such as seamounts, which influence vertical aggregation and predator–prey accessibility. The interaction and the relative importance of these factors vary seasonally and geographically and have a specific impact on the different communities.

Overall, the three regional systems considered span a spectrum of ecological configurations, which demonstrate the plasticity of pelagic ecosystems and their adaptability to different environmental conditions.

Finally, our study demonstrates that regional ecosystems are open systems that cannot be considered in isolation. The passive transport of biomass and the active movements that we highlight from 'source' regions, such as the HCS, to 'hub' regions, such as the PWP, or 'sink' regions, such as the SPG are functionally essential. This demonstrates the need to consider regional systems as interactive components of larger-scale, basin-wide dynamics.

4.3. Scope and limitations

In this paper we have demonstrated the ability of APECOSM to reproduce observed ecosystem configurations in three ecologically contrasting marine regions. The model has enabled the identification of the processes that underpin region-specific ecological structures and functions. The interaction of diverse environmental drivers with the elementary processes represented at the individual level in the model enables ecosystems to self-organise and adapt to environmental constraints, dissipating energy as efficiently as the interaction between environmental features and their biological and ecological constraints allows.

Despite these strengths, several limitations must be acknowledged. First, the use of a coarse, 1° resolution grid limits the model's ability to resolve fine-scale hydrodynamic features, particularly in the HCS, where key meso-scale and submeso-scale structures such as upwelling filaments, eddies, and retention cells play a critical role in shaping productivity and predator aggregation. Similarly, in the PWP, the ecological effects of complex island and seamount topographies, including localised upwellings, are oversimplified (see Fig. 6c). This compromises the representation of localised physical and biogeochemical processes and their cascading effects on both LTL and HTL communities.

In addition, oceanic ecosystems, such as the SPG, remain undersampled due to their remoteness and the low economic profitability of their fisheries. Opportunities for empirical evaluation of the model are therefore limited. In this data-poor context, APECOSM could serve as a tool to improve system-level understanding, propose hypotheses, and guide targeted observational studies.

Finally, the realism of APECOSM outputs is partly shaped by the underlying physical–biogeochemical forcing. For example, the PISCES model under-represents the horizontal extent of the eastern tropical Pacific OMZ, confining it to coastal zones, whereas observational data reveal a much broader hypoxic region (Garcia et al., 2019; Abe and Minobe, 2023; Takano et al., 2023). This mismatch directly influences the modelled spatial distribution and behaviour of OMZ-sensitive mesopelagic organisms, especially mesopelagic residents.

4.4. Perspectives

APECOSM offers a robust mechanistic framework for unravelling the complex three-dimensional structure and function of marine HTL communities. Together with the global-scale analysis of Dalaut et al. (2025), the present regional analyses provides a detailed understanding of the mechanisms influencing present HTL ecosystems. It offers foundations for future analyses of climate change impacts on pelagic ecosystems, and how marine food webs may reorganise under projected warming, deoxygenation, and primary production changes.

CRediT authorship contribution statement

Laureline Dalaut: Writing – review & editing, Writing – original draft, Visualization, Validation, Software, Formal analysis, Data curation, Conceptualization. **Nicolas Barrier:** Software, Data curation. **Matthieu Lengaigne:** Writing – review & editing, Supervision. **Olivier Maury:** Writing – review & editing, Validation, Supervision, Software, Methodology, Investigation, Conceptualization.

Declaration of competing interest

The authors declare the following financial interests/personal relationships which may be considered as potential competing interests: Laureline Dalaut reports financial support was provided by Programme Prioritaire Océan et Climat. If there are other authors, they declare that they have no known competing financial interests or personal relationships that could have appeared to influence the work reported in this paper.

Acknowledgement

LD is funded by Programme Prioritaire Océan et Climat (PPR, grant ANR n°22-POCE-0001).

Appendix A. Supplementary materials : Diet

Figure Fig. 10 shows details of the community diet across different sizes and regions.

Appendix B. Supplementary materials : Schooling

Figure Fig. 11 shows the probability of community schooling across different transects.

Appendix C. Supplementary materials : Trophic fluxes

Figure Fig. 12 details the trophic fluxes per community and size across different regions.

Appendix D. Supplementary materials : Biomass transport tendency terms

Figs. 13 and 14 show the transport tendency terms, which measure the cumulative effect of passive biomass transport by marine currents, as well as active movements, on regional biomass evolution. These terms are useful for isolating the effects of transport (including advective and diffusive components) from the effects of other processes affecting local biomass evolution such as growth, reproduction and mortality. As regional biomass is approximately stationary, the sum of all tendency terms averages to zero. Regions that exhibit a positive trend in transport tendency terms over time (i.e. a net biomass accumulation due to transport and movement) are 'sink' systems. In these systems, the community biomass growth rate is insufficient to maintain biomass stationarity without import. Communities can only persist in these 'sink' regions through sustained immigration from more productive 'source' systems (Pulliam, 1988). 'Source' ecosystems can be identified in Fig. 13 by their net export of biomass over time (negative transport tendency terms).

Appendix E. Supplementary materials : Shannon–Weaver index and interaction strength

To quantify the diversity of the simulated trophic networks, we calculated the Shannon–Weaver index H', a widely used metric for measuring species diversity derived from the information theory (Clarke and Warwick, 2001; Shannon and Weaver, 1949). The Shannon–Weaver index assumes that individuals are randomly sampled from a large population, and that all the species are represented in the sample (Shannon and Weaver, 1949). This index, applied to trophic flux in this paper, quantifies both richness (i.e. the number of links) and evenness (their commonness) of fluxes:

$$H = -\sum_{i=1}^{S} p_i \ln(p_i)$$

where:

- S is the total number of trophic links,
- $p_i = \frac{\text{flux}_i}{\text{total flux}}$ is the relative contribution of flux i.

To complement this, we computed the interaction strength F, representing the average intensity of matter or energy flows between trophic levels. Bronstein (1994), Thompson and Fernandez (2006):

$$F = \frac{1}{L} \sum_{(i,j)} |f_{ij}|$$

where:

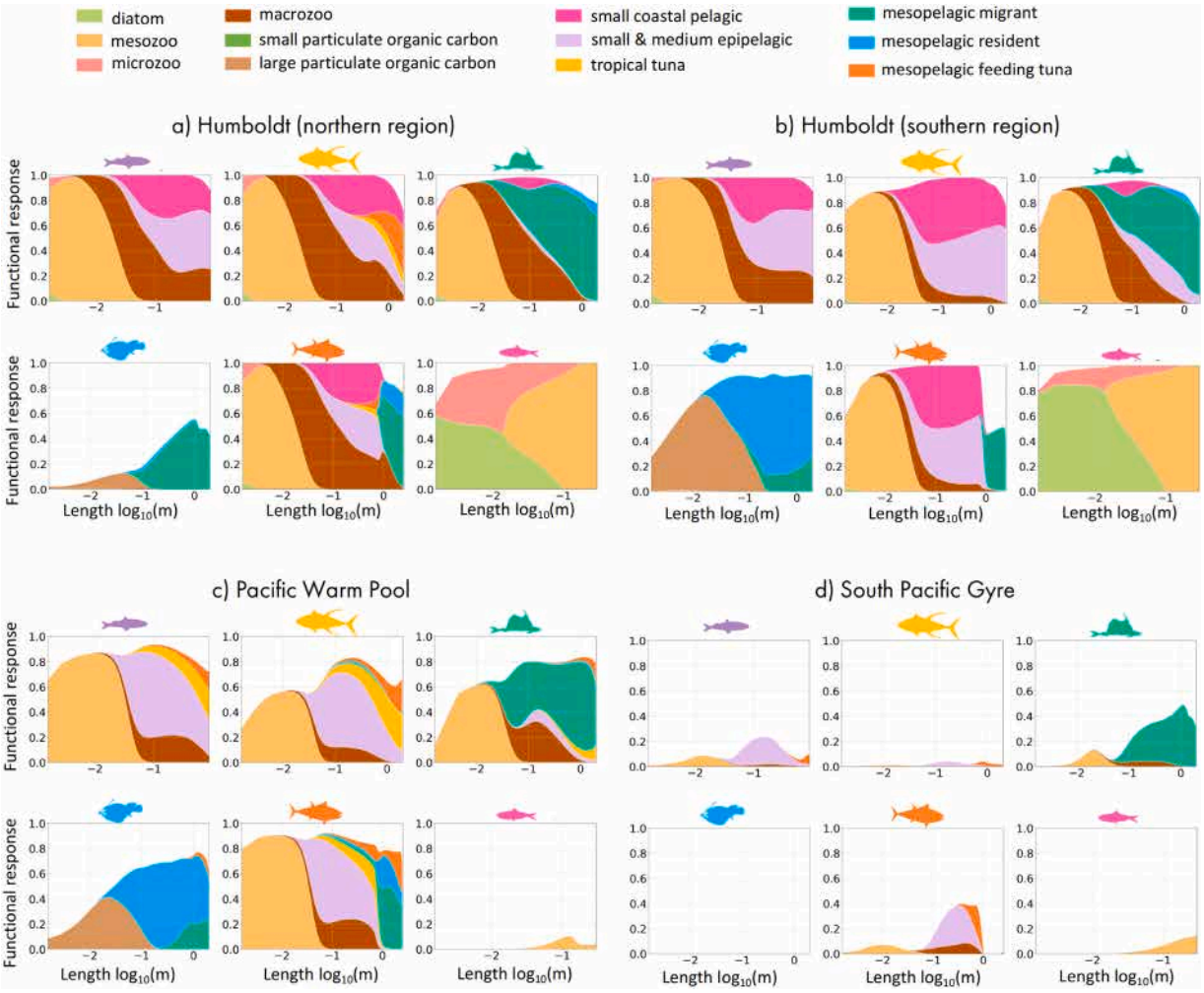

Fig. 10. Diet across regions. Community diets represent the relative proportions of the different food components in the diet of an individual predator of a given size and community, relative to satiation (which occurs when the functional response equals 1). The figures present the average diets from 2000 to 2020. Diet depends on the spatial (3D) co-occurrence of predators and prey, their size ratio, and the aggregation (schooling) and visibility of prey.

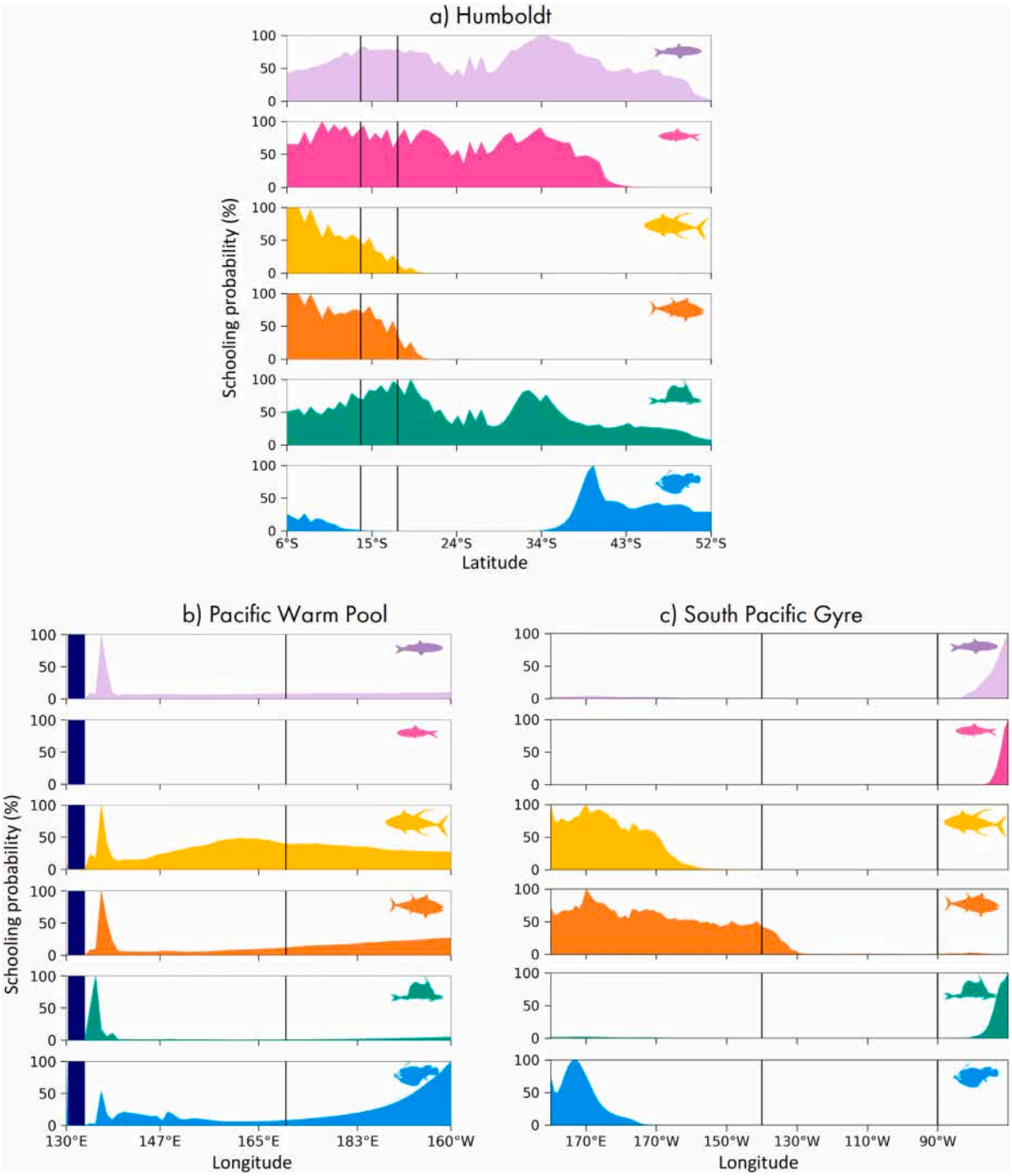

Fig. 11. Schooling across regions. The community schooling probability is shown along the different transects for each community. The values are averaged over the period 2000–2020 and integrated across all size classes and depth levels for the six APECOSM communities.

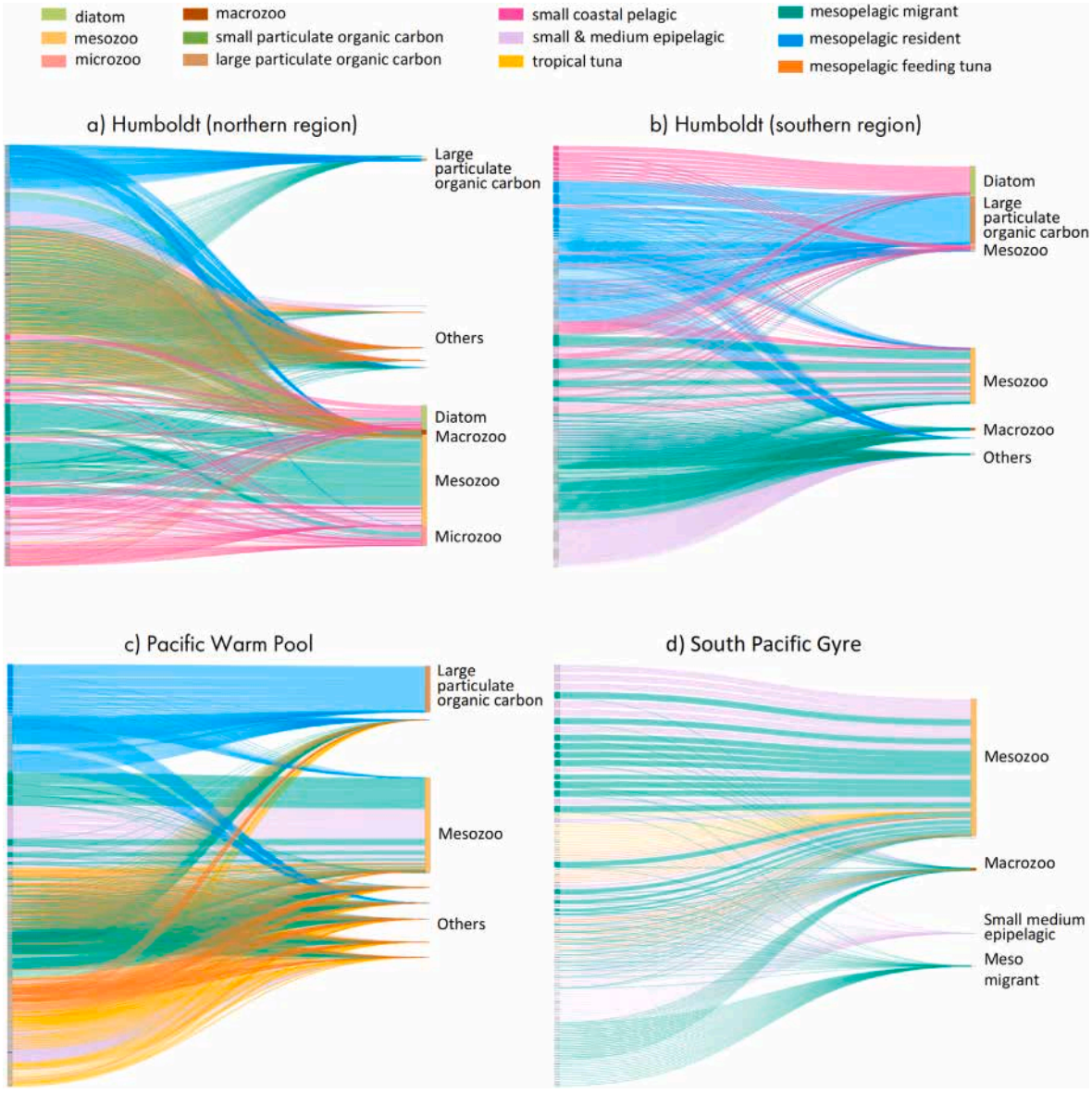

Fig. 12. Trophic fluxes across regions. Yearly trophic fluxes to HTL communities and size classes in each region. The left axis shows the HTL predators and the right axis shows the LTL (from PISCES) and HTL (from APECOSM) prey. The width of the connector is proportional to the energy flux ($J.yr^{-1}$) and is colour-coded according to the predator group. Values are averaged over 2000–2020.

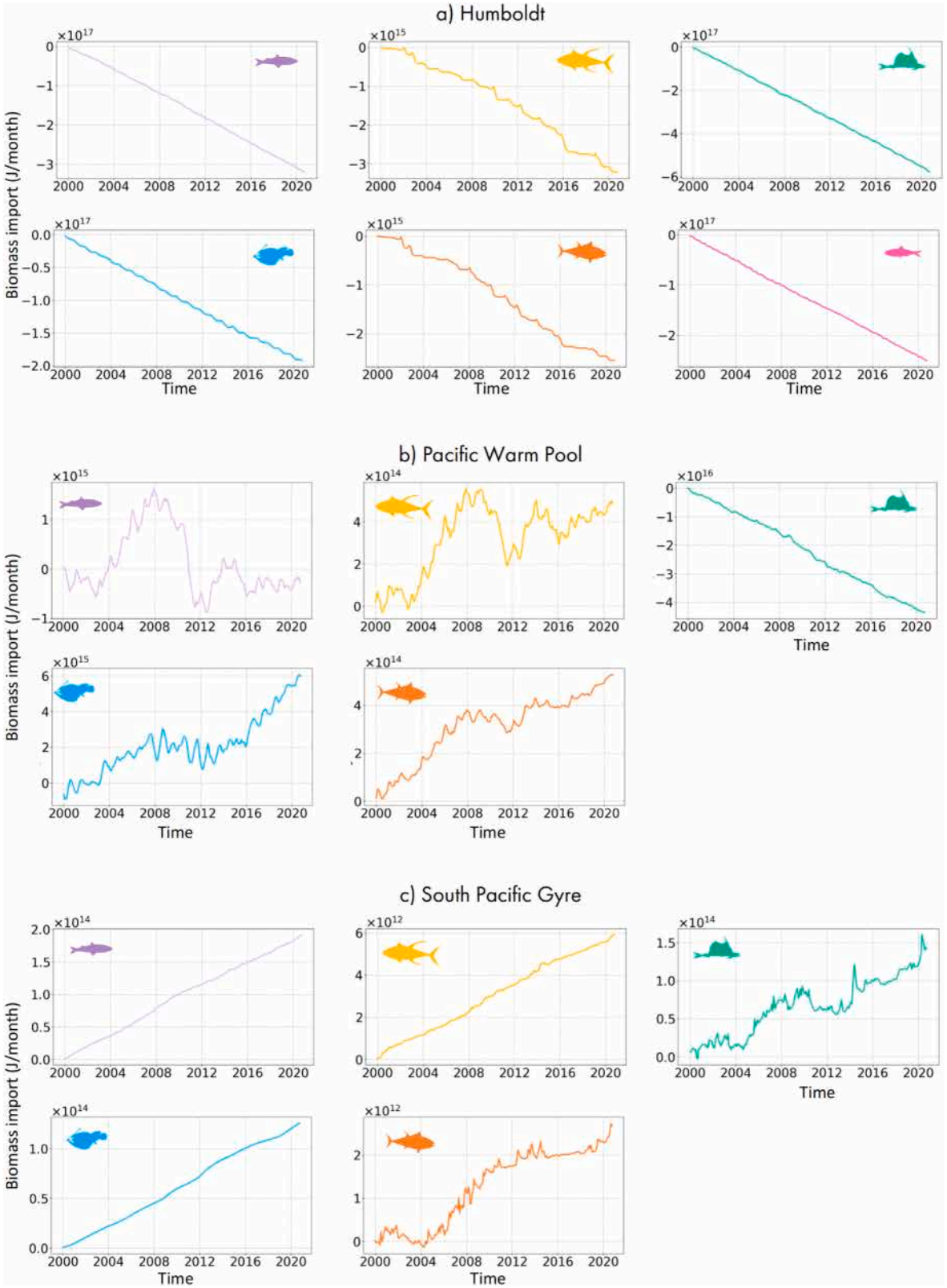

Fig. 13. Transport tendency terms across regions. Cumulative tendency terms sum the net biomass import (when positive, export when negative) resulting from passive and active, advective and diffusive movements for each community between 2000 and 2020 . These values sum zonal and meridional biomass import and export.

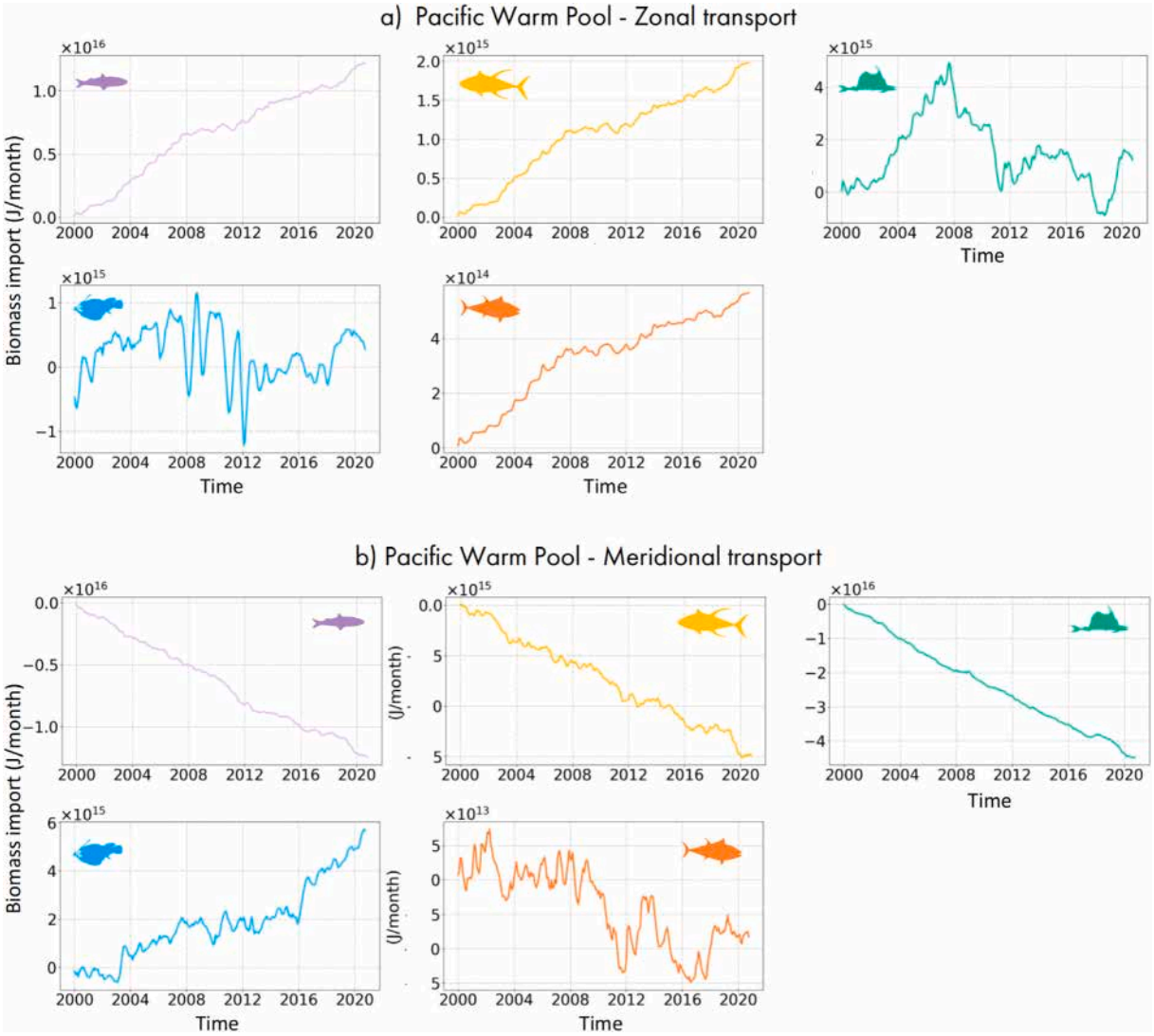

Fig. 14. Cumulative zonal and meridional transport tendency terms in the Pacific Warm Pool. (a) shows the cumulative transport tendency term (net biomass import) resulting from zonal passive and active, advective and diffusive movement. (b) shows the cumulative transport tendency terms (net biomass import) resulting from meridional transport. Transport tendency terms are shown for every community present in the region and evaluated between 2000 and 2020.

- L is the total number of links,
- f_{ij} is the strength of the trophic flux from node i to node j,
- $|f_{ij}|$ denotes the absolute value of the interaction strength.

Appendix F. Supplementary materials : Output data and Python scripts

Aggregated output data and Python scripts used for the figures are available online at: 10.5281/zenodo.16759655

Data availability

Data will be made available on request.

References

Abe, Y., Minobe, S., 2023. Comparison of ocean deoxygenation between CMIP models and an observational dataset in the north Pacific from 1958 to 2005. Front. Mar. Sci. 10, http://dx.doi.org/10.3389/fmars.2023.1161451.

AFMA, 2022. Small Pelagic Fishery : Management Arrangements Booklet 2023-24. Technical Report, Australian Fisheries Management Authority, Canberra, Australia.

Alheit, J., Niquen, M., 2004. Regime shifts in the humboldt current ecosystem. Prog. Oceanogr. 60 (2–4), 201–222. http://dx.doi.org/10.1016/j.pocean.2004.02.006.

Allain, V., Pilling, G.M., Williams, P.G., Harley, S., Nicol, S., Hampton, J., 2016. Overview of tuna Fisheries, stock status and management framework in the western and central Pacific ocean. In: Pauwels, S., Fache, E. (Eds.), Fisheries in the Pacific : the Challenges of Governance and Sustainability. In: Cahiers Du Credo, pacific-credo Publications, Marseille, pp. 19–48. http://dx.doi.org/10.4000/books.pacific.423.

Andersen, K.H., Berge, T., Gonçalves, R.J., Hartvig, M., Heuschele, J., Hylander, S., Jacobsen, N.S., Lindemann, C., Martens, E.A., Neuheimer, A.B., Olsson, K., Palacz, A., Prowe, A.E.F., Sainmont, J., Traving, S.J., Visser, A.W., Wadhwa, N., Kiørboe, T., 2016. Characteristic sizes of life in the oceans, from bacteria to whales. Annu. Rev. Mar. Sci. 8, 217–241. http://dx.doi.org/10.1146/annurev-marine-122414-034144.

Andréfouët, S., Adjeroud, M., 2019. French polynesia. In: World Seas: An Environmental Evaluation. Elsevier, pp. 827–854. http://dx.doi.org/10.1016/B978-0-08-100853-9.00039-7.

Annasawmy, P., Ternon, J.-F., Cotel, P., Cherel, Y., Romanov, E.V., Roudaut, G., Lebourges-Dhaussy, A., Ménard, F., Marsac, F., 2019. Micronekton distributions and assemblages at two shallow seamounts of the south-western Indian ocean: Insights from acoustics and mesopelagic trawl data. Prog. Oceanogr. 178, 102161. http://dx.doi.org/10.1016/j.pocean.2019.102161.

Antezana, T., 2009. Species-specific patterns of diel migration into the oxygen minimum zone by euphausiids in the humboldt current ecosystem. Prog. Oceanogr. 83 (1), 228–236. http://dx.doi.org/10.1016/j.pocean.2009.07.039.

Aracena, C., Lange, C.B., Luis Iriarte, J., Rebolledo, L., Pantoja, S., 2011. Latitudinal patterns of export production recorded in surface sediments of the Chilean

patagonian fjords (41–55°s) as a response to water column productivity. Cont. Shelf Res. 31 (3–4), 340–355. http://dx.doi.org/10.1016/j.csr.2010.08.008.

Armengol, L., Calbet, A., Franchy, G., Rodríguez-Santos, A., Hernández-León, S., 2019. Planktonic food web structure and trophic transfer efficiency along a productivity gradient in the tropical and subtropical Atlantic Ocean. Sci. Rep. 9 (1), 2044. http://dx.doi.org/10.1038/s41598-019-38507-9.

Aumont, O., Ethé, C., Tagliabue, A., Bopp, L., Gehlen, M., 2015. PISCES-v2: An ocean biogeochemical model for carbon and ecosystem studies. Geosci. Model. Dev. 8 (8), 2465–2513. http://dx.doi.org/10.5194/gmd-8-2465-2015.

Ayón, P., Swartzman, G., Bertrand, A., Gutiérrez, M., Bertrand, S., 2008. Zooplankton and forage fish species off Peru: Large-scale bottom-up forcing and local-scale depletion. Prog. Oceanogr. 79, 208–214. http://dx.doi.org/10.1016/j.pocean.2008.10.023.

Bakun, A., Weeks, S.J., 2008. The marine ecosystem off Peru: What are the secrets of its Fishery productivity and what might its future hold? Prog. Oceanogr. 79 (2), 290–299. http://dx.doi.org/10.1016/j.pocean.2008.10.027.

Barber, R.T., Chavez, F.P., 1991. Regulation of primary productivity rate in the equatorial Pacific. Limnol. Oceanogr. 36 (8), 1803–1815. http://dx.doi.org/10.4319/lo.1991.36.8.1803.

Barneche, D.R., Hulatt, C.J., Dossena, M., Padfield, D., Woodward, G., Trimmer, M., Yvon-Durocher, G., 2021. Warming impairs trophic transfer efficiency in a long-term field experiment. Nature 592 (7852), 76–79. http://dx.doi.org/10.1038/s41586-021-03352-2.

Barnett, M.A., 1983. Species structure and temporal stability of mesopelagic fish assemblages in the central gyres of the north and south Pacific ocean. Mar. Biol. 74 (3), 245–256. http://dx.doi.org/10.1007/BF00403448.

Barrier, N., Lengaigne, M., Rault, J., Person, R., Ethé, C., Aumont, O., Maury, O., 2023. Mechanisms underlying the epipelagic ecosystem response to ENSO in the equatorial Pacific ocean. Prog. Oceanogr. 213, 103002. http://dx.doi.org/10.1016/j.pocean.2023.103002.

Belgrano, A., Ursula M., S., Dunne, J., Ulanowicz, R.E., 2005. Aquatic Food Webs: An Ecosystem Approach, Andrea Belgrano, Ursula M.Scharler, Jennifer Dunne, Robert E. Ulanowicz OUP Oxford.

Bertrand, A., Chaigneau, A., Peraltilla, S., Ledesma, J., Graco, M., Monetti, F., Chavez, F.P., 2011. Oxygen: a fundamental property regulating pelagic ecosystem structure in the coastal southeastern tropical Pacific. PLoS One 6 (12), e29558. http://dx.doi.org/10.1371/journal.pone.0029558.

Bertrand, S., Díaz, E., Lengaigne, M., 2008a. Patterns in the spatial distribution of peruvian anchovy (*engraulis ringens*) revealed by spatially explicit fishing data. Prog. Oceanogr. 79 (2), 379–389. http://dx.doi.org/10.1016/j.pocean.2008.10.009.

Bertrand, A., Gerlotto, F., Bertrand, S., Gutiérrez, M., Alza, L., Chipollini, A., Díaz, E., Espinoza, P., Ledesma, J., Quesquén, R., Peraltilla, S., Chavez, F., 2008b. Schooling behaviour and environmental forcing in relation to anchoveta distribution: An analysis across multiple spatial scales. Prog. Oceanogr. 79 (2), 264–277. http://dx.doi.org/10.1016/j.pocean.2008.10.018.

Bi, R., Cao, Z., Ismar-Rebitz, S.M.H., Sommer, U., Zhang, H., Ding, Y., Zhao, M., 2021. Responses of marine diatom-dinoflagellate competition to multiple environmental drivers: Abundance, elemental, and biochemical aspects. Front. Microbiol. 12, http://dx.doi.org/10.3389/fmicb.2021.731786.

Blanchard, J.L., Heneghan, R.F., Everett, J.D., Trebilco, R., Richardson, A.J., 2017. From bacteria to whales: using functional size spectra to model marine ecosystems. Trends Ecol. Evolut. 32 (3), 174–186. http://dx.doi.org/10.1016/j.tree.2016.12.003.

Boehlert, G.W., Genin, A., 1987. A review of the effects of seamounts on biological processes. In: Seamounts, Islands, and Atolls. American Geophysical Union (AGU), pp. 319–334. http://dx.doi.org/10.1029/GM043p0319.

Borland, H.P., Gilby, B.L., Henderson, C.J., Leon, J.X., Schlacher, T.A., Connolly, R.M., Pittman, S.J., Sheaves, M., Olds, A.D., 2021. The influence of seafloor terrain on fish and Fisheries: A global synthesis. Fish Fish. 22 (4), 707–734. http://dx.doi.org/10.1111/faf.12546.

Broadhead, G.C., 1964. Some factors affecting the distribution and apparent abundance of yellowfin and skipjack tuna in the eastern Pacific ocean. SIDALC.

Bronstein, J.L., 1994. Conditional outcomes in mutualistic interactions. Trends Ecol. Evolut. 9 (6), 214–217. http://dx.doi.org/10.1016/0169-5347(94)90246-1.

Cavan, E.L., Trimmer, M., Shelley, F., Sanders, R., 2017. Remineralization of particulate organic carbon in an ocean oxygen minimum zone. Nat. Commun. 8 (1), 14847. http://dx.doi.org/10.1038/ncomms14847.

Cerna, F., Gómez, M., Moyano, G., Plaza, G., Morales-Nin, B., 2022. Spatial and inter-annual changes in the growth patterns of Young-of-year anchovy in a high productive ecosystem. Fish. Res. 249, 106236. http://dx.doi.org/10.1016/j.fishres.2022.106236.

Checkley, D.M., Asch, R.G., Rykaczewski, R.R., 2017. Climate, anchovy, and sardine. Annu. Rev. Mar. Sci. 9 (1), 469–493. http://dx.doi.org/10.1146/annurev-marine-122414-033819.

Childress, J.J., Seibel, B.A., 1998. Life at stable low oxygen levels: adaptations of animals to oceanic oxygen minimum layers. J. Exp. Biol. 201 (8), 1223–1232. http://dx.doi.org/10.1242/jeb.201.8.1223.

Clarke, K., Warwick, R., 2001. Clarke KR, Warwick RM.Change in Marine Communities: An Approach to Statistical Analysis and Interpretation, Natural Resources ed. Primer-E Ltd, Plymouth, UK.

Claustre, H., Huot, Y., Obernosterer, I., Gentili, B., Tailliez, D., Lewis, M., 2008. Gross community production and metabolic balance in the south Pacific gyre, using a non intrusive bio-optical method. Biogeosciences.

Coghlan, A.R., White, R., Dawson, T.P., Irving, R.A., Zeller, D., Palomares, M.L.D., 2017. Reconstructed marine Fisheries catches at a remote island group: Pitcairn Islands (1950–2014). Front. Mar. Sci. 4, http://dx.doi.org/10.3389/fmars.2017.00320.

Cornec, M., Claustre, H., Mignot, A., Guidi, L., Lacour, L., Poteau, A., D'Ortenzio, F., Gentili, B., Schmechtig, C., 2021. Deep chlorophyll maxima in the global ocean: Occurrences, drivers and characteristics. Glob. Biogeochem. Cycles 35 (4), e2020GB006759. http://dx.doi.org/10.1029/2020GB006759.

Cornejo, R., Koppelmann, R., 2006. Distribution patterns of mesopelagic fishes with special reference to vinciguerria lucetia garman 1899 (phosichthyidae: Pisces) in the Humboldt Current Region off peru. Mar. Biol. 149 (6), 1519–1537. http://dx.doi.org/10.1007/s00227-006-0319-z.

Cubillos, L., Serra, R., Fréon, P., 2007. Synchronous pattern of fluctuation in three anchovy Fisheries in the humboldt current system. 20, http://dx.doi.org/10.1051/alr:2007017.

Dai, M., Luo, Y.-W., Achterberg, E.P., Browning, T.J., Cai, Y., Cao, Z., Chai, F., Chen, B., Church, M.J., Ci, D., Du, C., Gao, K., Guo, X., Hu, Z., Kao, S.-J., Laws, E.A., Lee, Z., Lin, H., Liu, Q., Liu, X., Luo, W., Meng, F., Shang, S., Shi, D., Saito, H., Song, L., Wan, X.S., Wang, Y., Wang, W.-L., Wen, Z., Xiu, P., Zhang, J., Zhang, R., Zhou, K., 2023. Upper ocean biogeochemistry of the oligotrophic north Pacific subtropical gyre: from nutrient sources to carbon export. Rev. Geophys. 61 (3), e2022RG000800. http://dx.doi.org/10.1029/2022RG000800.

Dalaut, L., Barrier, N., Lengaigne, M., Rault, J., Ariza, A., Belharet, M., Brunel, A., Schwamborn, R., Travassos-Tolotti, M., Maury, O., 2025. Which processes structure global pelagic ecosystems and control their trophic functioning? insights from the mechanistic model APECOSM. Prog. Oceanogr. 235, 103480. http://dx.doi.org/10.1016/j.pocean.2025.103480.

De Deckker, P., 2016. The indo-Pacific warm pool: Critical to world oceanography and world climate. Geosci. Lett. 3 (1), 20. http://dx.doi.org/10.1186/s40562-016-0054-3.

Diaz, J., Miloslavich, P., Klein, E., Hernández, C., Bigatti, G., Artigas, F., Penchaszadeh, P., Diaz de Astarloa, J., Neill, P., Lewis, M., Rodriguez, D., 2013. Marine biodiversity in the atlantic and Pacific coasts of south america: knowledge and gaps.

Dubroca, L., Chassot, E., Floch, L., Demarcq, H., Assan, C., de Molina, A.D., 2014. Seamounts and tuna Fisheries : Tuna hotspots or Fishermen habits ? In: 2012 Inter-Sessional Meeting of the Tropical Tuna Species Group. p. 2087.

Echevin, V., Albert, A., Lévy, M., Graco, M., Aumont, O., Piétri, A., Garric, G., 2014. Intraseasonal variability of nearshore productivity in the northern humboldt current system: The role of coastal trapped waves. Cont. Shelf Res. 73, 14–30. http://dx.doi.org/10.1016/j.csr.2013.11.015.

Eduardo, L.N., Mincarone, M.M., Sutton, T., Bertrand, A., 2024. Deep-pelagic fishes are anything but similar: a global synthesis. Ecol. Lett. 27 (9), e14510. http://dx.doi.org/10.1111/ele.14510.

Eriksen, M., Maximenko, N., Thiel, M., Cummins, A., Lattin, G., Wilson, S., Hafner, J., Zellers, A., Rifman, S., 2013. Plastic pollution in the south Pacific subtropical gyre. Marine Poll. Bull. 68 (1), 71–76. http://dx.doi.org/10.1016/j.marpolbul.2012.12.021.

FAO, 2011. Fisheries of the Pacific Islands: Regional and National Information. Technical Report, FAO, Bangkok.

FAO, 2021. FAO Yearbook. Fishery and Aquaculture Statistics 2019 FAO. FAO, http://dx.doi.org/10.4060/cb7874t.

Farquhar, G.B., 1971. International Symposium on Biological Sound Scattering in the Ocean, Airlie House, 1970: Proceedings. U.S. Government Printing Office.

Fiedler, P.C., Lavín, M.F., 2017. Oceanographic conditions of the eastern tropical Pacific. In: Glynn, P.W., Manzello, D.P., Enochs, I.C. (Eds.), Coral Reefs of the Eastern Tropical Pacific: Persistence and Loss in a Dynamic Environment. Springer Netherlands, Dordrecht, pp. 59–83. http://dx.doi.org/10.1007/978-94-017-7499-4_3.

Fink, B.D., 1970. Migrations of yellowfin and skipjack tuna in the eastern Pacific ocean as determined by tagging experiments, 1952–1964. SIDALC.

Fock, H.O., Matthiessen, B., Zidowitz, H., v Westernhagen, H., 2002. Diel and habitat-dependent resource utilisation by deep-sea fishes at the great meteor seamount: Niche overlap and support for the sound scattering layer interception hypothesis. Mar. Ecol. Prog. Ser. 244, 219–233. http://dx.doi.org/10.3354/meps244219.

Fonteneau, A., 1991. Monts sous-marins et thons dans l'atlantique tropical est. Aquat. Living Resour. 4 (1), 13–25. http://dx.doi.org/10.1051/alr:1991001.

Fonteneau, A., 1997. Atlas des pêcheries thonières tropicales: captures mondiales et environnement. ORSTOM éditions, Paris.

Fuenzalida, R., Schneider, W., Garcés-Vargas, J., Bravo, L., Lange, C., 2009. Vertical and horizontal extension of the oxygen minimum zone in the eastern south Pacific ocean. Deep. Sea Res. Part II: Top. Stud. Ocean. 56 (16), 992–1003. http://dx.doi.org/10.1016/j.dsr2.2008.11.001.

Fujioka, K., Aoki, Y., Tsuda, Y., Okamoto, K., Tsuchida, H., Sasaki, A., Kiyofuji, H., 2024. Influence of temperature on hatching success of skipjack tuna (*katsuwonus pelamis*): implications for spawning availability of warm habitats. J. Fish Biol. jfb.15767. http://dx.doi.org/10.1111/jfb.15767.

Fuller, L., Griffiths, S., Olson, R., Galván-Magaña, F., Bocanegra-Castillo, N., Alatorre-Ramírez, V., 2021. Spatial and ontogenetic variation in the trophic ecology of skipjack tuna, katsuwonus pelamis, in the eastern Pacific ocean. Mar. Biol. 168 (5), 73. http://dx.doi.org/10.1007/s00227-021-03872-5.

Fulton, E., Smith, A., Johnson, C., 2003. Effect of complexity on marine ecosystem models. Mar. Ecol. Prog. Ser. 253, 1–16. http://dx.doi.org/10.3354/meps253001.

Garcia, H., Weathers, K., Paver, C., Smolyar, I., Boyer, T., Locarnini, M., Zweng, M., Mishonov, A., Baranova, O., Seidov, D., Reagan, J., Paver, C., Smolyar, I., Boyer, T., Locarnini, M., Zweng, M., Mishonov, A., Baranova, O., Seidov, D., Reagan, J., 2019. World ocean atlas 2018, volume 3: dissolved oxygen, apparent oxygen utilization, and dissolved oxygen saturation. In: World Ocean Atlas, vol. 3, NOAA Atlas NESDIS 83, p. 38.

Gjosaeter, J., 1984. Mesopelagic fish, a large potential resource in the arabian sea. Deep. Sea Res. Part A. Ocean. Res. Pap. 31 (6), 1019–1035. http://dx.doi.org/10.1016/0198-0149(84)90054-2.

Guiet, J., Poggiale, J.-C., Maury, O., 2016. Modelling the community size-spectrum: Recent developments and new directions. Ecol. Model. 337, 4–14. http://dx.doi.org/10.1016/j.ecolmodel.2016.05.015.

Halm, H., Lam, P., Ferdelman, T.G., Lavik, G., Dittmar, T., LaRoche, J., D'Hondt, S., Kuypers, M.M.M., 2012. Heterotrophic organisms dominate nitrogen fixation in the south Pacific gyre. ISME J. 6 (6), 1238–1249. http://dx.doi.org/10.1038/ismej.2011.182.

Hasan, M.R., Halwart, M., 2009. Fish as feed inputs for aquaculture: Practices, sustainability and implications. Number 518 in FAO Fisheries and Aquaculture Technical Paper, FAO, Rome.

Hill, M.N., 1963. The Sea, Volume 2: The Composition of Sea-Water; Comparative and Descriptive Oceanography. Harvard University Press.

Holland, K., Grubbs, R., 2007. Fish visitors to seamounts: Tunas and bill fish at seamounts. In: Seamounts: Ecology, Fisheries and Conservation. pp. 189–201. http://dx.doi.org/10.1002/9780470691953.ch10a.

Holland, K.N., Kleiber, P., Kajiura, S.M., 1999. Different residence times of yellowfin tuna, thunnus albacares, and bigeye tuna, T. Obesus, found in mixed aggregations over a seamount. Fish. Bull.-National Ocean. Atmos. Adm..

IATTC, 2022. The tuna Fishery in the EPO in 2022. Meeting Report 101-01, IATTC, Victoria, B.C., Canada.

Jennings, S., Mackinson, S., 2003. Abundance–body mass relationships in size-structured food webs. Ecol. Lett. 6 (11), 971–974. http://dx.doi.org/10.1046/j.1461-0248.2003.00529.x.

Kämpf, J., Chapman, P., 2016. The peruvian-Chilean coastal upwelling system. In: Kämpf, J., Chapman, P. (Eds.), Upwelling Systems of the World: a Scientific Journey To the Most Productive Marine Ecosystems. Springer International Publishing, Cham, pp. 161–201. http://dx.doi.org/10.1007/978-3-319-42524-5_5.

Karcher, D.B., Fache, E., Breckwoldt, A., Govan, H., Elías Ilosvay, X.E., Kam King, J.K., Riera, L., Sabinot, C., 2020. Trends in south Pacific Fisheries management. Mar. Policy 118, 104021. http://dx.doi.org/10.1016/j.marpol.2020.104021.

Karstensen, J., Ulloa, O., 2009. Peru–Chile current system. In: Encyclopedia of Ocean Sciences. pp. 385–392. http://dx.doi.org/10.1016/B978-012374473-9.00599-3.

Klimley, A.P., 1993. Highly directional swimming by scalloped hammerhead sharks, sphyrna lewini, and subsurface irradiance, temperature, bathymetry, and geomagnetic field. Mar. Biol. 117 (1), 1–22. http://dx.doi.org/10.1007/BF00346421.

Klimley, A.P., Jorgensen, S.J., Muhlia-Melo, A., Beavers, S.C., 2003. The occurrence of yellowfin tuna (thunnus albacares) at espiritu santo seamount in the Gulf of California. Fish. Bull..

Kobayashi, S., Ota, Y., Harada, Y., Ebita, A., Moriya, M., Onoda, H., Onogi, K., Kamahori, H., Kobayashi, C., Endo, H., Miyaoka, K., Takahashi, K., 2015. The JRA-55 reanalysis: general specifications and basic characteristics. J. Meteorol. Soc. Jpn. Ser. II 93 (1), 5–48. http://dx.doi.org/10.2151/jmsj.2015-001.

Kong, L.F., He, Y.B., Xie, Z.X., Luo, X., Zhang, H., Yi, S.H., Lin, Z.L., Zhang, S.F., Yan, K.Q., Xu, H.K., Jin, T., Lin, L., Qin, W., Chen, F., Liu, S.Q., Wang, D.Z., 2021. Illuminating key microbial players and metabolic processes involved in the remineralization of particulate organic carbon in the ocean's twilight zone by metaproteomics. Appl. Environ. Microbiol. 87 (20), e00986–21. http://dx.doi.org/10.1128/AEM.00986-21.

Kooijman, B., 2010. Dynamic Energy Budget Theory for Metabolic Organisation, third ed. Cambridge University Press, Cambridge, http://dx.doi.org/10.1017/CBO9780511805400.

Langley, A., Adams, T., 2005. The potential for development of Fisheries in the pitcairn EEZ.

Langley, A., Wright, A., Hurry, G., Hampton, J., Aqorua, T., Rodwell, L., 2009. Slow steps towards management of the world's largest tuna Fishery. Mar. Policy 33 (2), 271–279. http://dx.doi.org/10.1016/j.marpol.2008.07.009.

Le Mézo, P., Lefort, S., Séférian, R., Aumont, O., Maury, O., Murtugudde, R., Bopp, L., 2016. Natural variability of marine ecosystems inferred from a coupled climate to ecosystem simulation. J. Mar. Syst. 153, 55–66. http://dx.doi.org/10.1016/j.jmarsys.2015.09.004.

Lengaigne, M., Pang, S., Silvy, Y., Danielli, V., Gopika, S., Sadhvi, K., Rousset, C., Ethé, C., Person, R., Madec, G., Barrier, N., Maury, O., Menkes, C., Nicol, S., Gorgues, T., Melet, A., Guihou, K., Vialard, J., Silvy, Y., Danielli, V., Gopika, S., Sadhvi, K., Rousset, C., Ethé, C., Person, R., Madec, G., Barrier, N., Maury, O., Menkes, C., Nicol, S., Gorgues, T., Melet, A., Guihou, K., Vialard, J., 2024. An ocean-only framework for correcting future CMIP oceanic projections from their present-day biases. ESS Open Arch. http://dx.doi.org/10.22541/essoar.172019498.89258365/v1.

Longhurst, A., Sathyendranath, S., Platt, T., Caverhill, C., 1995. An estimate of global primary production in the ocean from satellite radiometer data. J. Plankton Res. 17 (6), 1245–1271. http://dx.doi.org/10.1093/plankt/17.6.1245.

Madec, G., 2015. NEMO Ocean Engine. Technical Report, Institut Pierre-Simon Laplace, Institut Pierre-Simon Laplace.

Mashayek, A., Gula, J., Baker, L.E., Naveira Garabato, A.C., Cimoli, L., Riley, J.J., de Lavergne, C., 2024. On the role of seamounts in upwelling deep-ocean waters through turbulent mixing. Proc. Natl. Acad. Sci. 121 (27), e2322163121. http://dx.doi.org/10.1073/pnas.2322163121.

Maury, O., 2010. An overview of APECOSM, a spatialized mass balanced "apex predators ecosystem model" to study physiologically structured tuna population dynamics in their ecosystem. Prog. Oceanogr. 84 (1–2), 113–117. http://dx.doi.org/10.1016/j.pocean.2009.09.013.

Maury, O., 2017. Can schooling regulate marine populations and ecosystems? Prog. Oceanogr. 156, 91–103. http://dx.doi.org/10.1016/j.pocean.2017.06.003.

Maury, O., Poggiale, J.C., 2013. From individuals to populations to communities: A dynamic energy budget model of marine ecosystem size-spectrum including life history diversity. J. Theoret. Biol. 324, 52–71. http://dx.doi.org/10.1016/j.jtbi.2013.01.018.

Maury, O., Shin, Y.J., Faugeras, B., Ben Ari, T., Marsac, F., 2007. Modeling environmental effects on the size-structured energy flow through marine ecosystems. part 2: simulations. Prog. Oceanogr. 74, 500–514. http://dx.doi.org/10.1016/j.pocean.2007.05.001.

Misselis, C., Ponsonnet, C., 2015. La pêche hauturière pélagique et démersale autour de l'archipel des australes. In: Environnement marin des îles Australes (Polynésie française), The Pew Charitable Trusts, Institut des Récifs Coralliens de l'ephe ed. p. 69.

Moore, B.R., Bell, J.D., Evans, K., Farley, J., Grewe, P.M., Hampton, J., Marie, A.D., Minte-Vera, C., Nicol, S., Pilling, G.M., Scutt Phillips, J., Tremblay-Boyer, L., Williams, A.J., Smith, N., 2020. Defining the stock structures of key commercial tunas in the Pacific Ocean I: Current knowledge and main uncertainties. Fish. Res. 230, 105525. http://dx.doi.org/10.1016/j.fishres.2020.105525.

Moore, J.A., Vecchione, M., Gibbons, R., Galbraith, J.K., Turnipseed, M., Southworth, M., Watkins, E., 2003. Biodiversity of bear seamount, new England seamount chain: results of exploratory trawling. J. Northwest Atl. Fish. Sci. 31, 363–372.

Musyl, M.K., Brill, R.W., Boggs, C.H., Curran, D.S., Kazama, T.K., Seki, M.P., 2003. Vertical movements of bigeye tuna (thunnus obesus) associated with islands, buoys, and seamounts near the main hawaiian islands from archival tagging data. Fisheries Oceanography 12 (3), 152–169. http://dx.doi.org/10.1046/j.1365-2419.2003.00229.x.

Parin, N., Mironov, A., Nesis, K., 1997. Biology of the nazca and sala y gòmez submarine ridges, an outpost of the indo-west Pacific fauna in the eastern Pacific ocean: composition and distribution of the fauna, its communities and history. In: Advances in Marine Biology, vol. 32, Elsevier, pp. 145–242. http://dx.doi.org/10.1016/S0065-2881(08)60017-6.

Parin, N.V., Prut'ko, V.G., 1985. The thalassial mesobenthopelagic ichthyocoene above the equator seamount in the western tropical Indian ocean. Oceanology 25 (6), 781–783.

Pennington, J.T., Mahoney, K.L., Kuwahara, V.S., Kolber, D.D., Calienes, R., Chavez, F.P., 2006. Primary production in the eastern tropical Pacific: A review. Prog. Oceanogr. 69 (2–4), 285–317. http://dx.doi.org/10.1016/j.pocean.2006.03.012.

Pizarro, O., Shaffer, G., Dewitte, B., Ramos, M., 2002. Dynamics of seasonal and interannual variability of the peru-Chile undercurrent. Geophys. Res. Lett. 29 (12), 22–1–22–4. http://dx.doi.org/10.1029/2002GL014790.

Pulliam, H.R., 1988. Sources, sinks, and population regulation. Amer. Nat. http://dx.doi.org/10.1086/284880.

Pusch, C., Beckmann, A., Porteiro, F.M., 2004. The influence of seamounts on mesopelagic fish communities. Arch. Fish. Mar. Res..

Radenac, M.H., Messié, M., Léger, F., Bosc, C., 2013. A very oligotrophic zone observed from space in the equatorial Pacific warm pool. Remote Sens. Environ. 134, 224–233. http://dx.doi.org/10.1016/j.rse.2013.03.007.

Reid, J.L., 1986. On the total geostrophic circulation of the south Pacific ocean: flow patterns, tracers and transports. Prog. Oceanogr. 16 (1), 1–61. http://dx.doi.org/10.1016/0079-6611(86)90036-4.

Ridgway, K.R., Dunn, J.R., 2003. Mesoscale structure of the mean east Australian current system and its relationship with topography. Prog. Oceanogr. 56 (2), 189–222. http://dx.doi.org/10.1016/S0079-6611(03)00004-1.

Ridgway, K., Hill, K., 2009. The east Australian current. In: Poloczanska, E.S., Hobday, A.J., Richardson, A.J. (Eds.), A Marine Climate Change Impacts and Adaptation Report Card for Australia 2009. NCCARF Publication, p. 12.

Roemmich, D., Gilson, J., Sutton, P., Zilberman, N., 2016. Multidecadal change of the south Pacific gyre circulation. J. Phys. Oceanogr. 46 (6), 1871–1883. http://dx.doi.org/10.1175/JPO-D-15-0237.1.

Rogers, A.D., 2018. Chapter four - the biology of seamounts: 25 years on. In: Sheppard, C. (Ed.), In: Advances in Marine Biology, vol. 79, Academic Press, pp. 137–224. http://dx.doi.org/10.1016/bs.amb.2018.06.001.

Rossberg, A.G., Gaedke, U., Kratina, P., 2019. Dome patterns in pelagic size spectra reveal strong trophic cascades. Nat. Commun. 10 (1), 4396. http://dx.doi.org/10.1038/s41467-019-12289-0.

Schneider, W., Fukasawa, M., Garcés-Vargas, J., Bravo, L., Uchida, H., Kawano, T., Fuenzalida, R., 2007. Spin-up of south Pacific subtropical gyre freshens and cools the upper layer of the eastern south Pacific ocean. Geophys. Res. Lett. 34 (24), http://dx.doi.org/10.1029/2007GL031933.

Seibel, B.A., 2011. Critical oxygen levels and metabolic suppression in oceanic oxygen minimum zones. J. Exp. Biol. 214 (2), 326–336. http://dx.doi.org/10.1242/jeb.049171.

Shannon, C.E., Weaver, W., 1949. The Mathematical Theory of Communication. University of Illinois Press, Champaign, IL, US, p. vi, 117.

Soviadan, Y.D., Benedetti, F., Brandão, M.C., Ayata, S.D., Irisson, J.O., Jamet, J.L., Kiko, R., Lombard, F., Gnandi, K., Stemmann, L., 2022. Patterns of mesozooplankton community composition and vertical fluxes in the global ocean. Prog. Oceanogr. 200, 102717. http://dx.doi.org/10.1016/j.pocean.2021.102717.

Takano, Y., Ilyina, T., Tjiputra, J., Eddebbar, Y.A., Berthet, S., Bopp, L., Buitenhuis, E., Butenschön, M., Christian, J.R., Dunne, J.P., Gröger, M., Hayashida, H., Hieronymus, J., Koenigk, T., Krasting, J.P., Long, M.C., Lovato, T., Nakano, H., Palmieri, J., Schwinger, J., Séférian, R., Suntharalingam, P., Tatebe, H., Tsujino, H., Urakawa, S., Watanabe, M., Yool, A., 2023. Simulations of ocean deoxygenation in the historical era: Insights from forced and coupled models. Front. Mar. Sci. 10, http://dx.doi.org/10.3389/fmars.2023.1139917.

Thiel, M., Macaya, E., Acuna, E., Arntz, W., Bastias, H., Brokordt, K., Camus, P., Castilla, J., Castro, L., Cortes, M., Dumont, C., Escribano, R., Fernandez, M., Gajardo, J., Gaymer, C., Gomez, I., Gonzalez, A., González, H., Haye, P., Vega, J.M.A., 2007. The humboldt current system of northern and central Chile. Ocean. Mar. Biol. 45, 195–345.. http://dx.doi.org/10.1201/9781420050943.ch6.

Thompson, J.N., Fernandez, C.C., 2006. Temporal dynamics of antagonism and mutualism in a geographically variable plant–insect interaction. Ecology 87 (1), 103–112. http://dx.doi.org/10.1890/05-0123.

Tornquist, F., Bigg, G.R., Bryant, R.G., 2024. Physical mechanisms affecting phytoplankton variability along the Chilean coast. J. Mar. Syst. 242, 103934. http://dx.doi.org/10.1016/j.jmarsys.2023.103934.

Urmy, S.S., Horne, J.K., Barbee, D.H., 2012. Measuring the vertical distributional variability of pelagic fauna in Monterey bay. ICES J. Mar. Sci. 69 (2), 184–196. http://dx.doi.org/10.1093/icesjms/fsr205.

Valdés, J., Sifeddine, A., Guiñez, M., Castillo, A., 2021. Oxygen minimum zone variability during the last 700 years in a coastal upwelling area of the humboldt system (mejillones, 23° s, Chile). A new approach from geochemical signature. Prog. Oceanogr. 193, 102520. http://dx.doi.org/10.1016/j.pocean.2021.102520.

Williams, P., Terawasi, P., 2009. Overview of Tuna Fisheries in the Western and Central Pacific Ocean, Including Economic Conditions. Technical Report WCPFC-SC6-2010/GN WP-1, Western and central Pacific Fisheries Commission.

Wishner, K.F., Ashjian, C.J., Gelfman, C., Gowing, M.M., Kann, L., Levin, L.A., Mullineaux, L.S., Saltzman, J., 1995. Pelagic and benthic ecology of the lower interface of the eastern tropical Pacific oxygen minimum zone. Deep. Sea Res. Part I: Ocean. Res. Pap. 42 (1), 93–115. http://dx.doi.org/10.1016/0967-0637(94)00021-J.

Wishner, K.F., Gowing, M.M., Gelfman, C., 1998. Mesozooplankton biomass in the upper 1000m in the arabian sea: Overall seasonal and geographic patterns, and relationship to oxygen gradients. Deep. Sea Res. Part II: Top. Stud. Ocean. 45 (10–11), 2405–2432. http://dx.doi.org/10.1016/S0967-0645(98)00078-2.

Yapur-Pancorvo, A.L., Quispe-Machaca, M., Guzmán-Rivás, F., Urzúa, Á., Espinoza, P., 2023. The red squat lobster pleuroncodes monodon in the humboldt current system: from their ecology to commercial attributes as marine bioresource. Animals 13 (14), 2279. http://dx.doi.org/10.3390/ani13142279.

Young, J.W., Hobday, A.J., Campbell, R.A., Kloser, R.J., Bonham, P.I., Clementson, L.A., Lansdell, M.J., 2011. The biological oceanography of the east Australian current and surrounding waters in relation to tuna and billfish catches off eastern Australia. Deep. Sea Res. Part II: Top. Stud. Ocean. 58 (5), 720–733. http://dx.doi.org/10.1016/j.dsr2.2010.10.005.

Zylich, K., Harper, S., Licandeo, R., Vega, R., Zeller, D., Pauly, D., 2014. Fishing in easter island, a recent history (1950 2010). Lat. Am. J. Aquat. Res. 42 (4), 845–856. http://dx.doi.org/10.3856/vol42-issue4-fulltext-11.